POLITECNICO

MILANO 1863

Procedural Generation of DOOM Levels

TESI DI LAUREA MAGISTRALE IN
INGEGNERIA INFORMATICA

Author: **Akash Aloysius James**

Student ID: 10687690
Advisor: Danielé Loiacono
Co-advisors: Pierluca Lanzi
Academic Year: 2022-23

Abstract

This study examines how to automate the process of populating procedurally generated levels using Conditional Adversarial Networks. The goal is to spawn game objects in a manner that functionally mimics the characteristics of those present in human designed levels without the need to explicitly define an exhaustive set of rules to govern the system. It is meant to enhance the level building process proposed in the work by upgrading the process of including content within the generated DOOM levels. The initial objective is to produce a coherent topology, accompanied by a suitable availability and positioning of game objects with respect to the level layout. This requires addressing complications that impede consistent representation and generation from the precious design. Then the modifications are compiled together to fashion a generative system that can construct the minimum sufficient subset of features used to design a unique level. Finally, a comparison is made between the modified system and the prior architecture to highlight the improvements it provides in regard to what was previously feasible. These samples are evaluated in a manner that contrasts the differences present among them and those available in the repository. The outcome of these experiments should prove a degree of competence in the system's ability for level design and act as a practical alternative for the implementation of procedural content generation for games to come.

Contents

1 | Introduction

The perceived value of video games as a recreational activity is deeply rooted in the duration and intensity that they manage to keep players engaged. A few decades ago, as fewer games were released within any given period, developers would often try to prolong gameplay to validate the costs. This was achieved with irregular difficulty spikes and by concealing information which coupled with the absence of the ability to retrieve one's progress, would cause players to take several months to complete. In comparison, despite numerous technological advances and man hours put into creating vast maps and longer stories, games today can be completed much sooner. This is partly due to adjustable difficulty, save points and widely available walkthroughs, thereby providing a shorter gameplay at a significant cost. The novelty also quickly wears off on repeated playthroughs and feels monotonous, especially when there are limited to no variations in gameplay, affecting a game's ability to retain players engagement over longer durations.

Replayability is the player's desire to continue playing a game even after experiencing the content, either to optimize one's skill or to explore its hidden content. It is beneficial as this kind of dedication arises from player satisfaction and has been shown to improve brand loyalty [7], yet many studios struggle to meet these expectations. This is usually attributed to the difficulty in maintaining player engagement over repeated sessions as it is critical that players don't know how every aspect of any level has been laid out. Some of the ways used to tackle this are by bringing in competitive aspects such as leaderboards or regular introduction of new content through updates which is made use of by many MMORPGs in order to maintain an active player base. The focus of this thesis is to address this problem by avoiding the monotony of traversing the same level through variations introduced in the level design.

1.1.   Background

An approach that has long been resorted to combat repetitiveness in replay is procedural generation. Early adopters of the technology include games such as Rogue [35] with its procedurally generated dungeon and the trading game Elite [3], where each of its planets had randomly determined compositions. The former has spawned its own genre called 'roguelike' that initially used a similar tile-based procedural system. The notion of randomly generating levels solely utilizing existing assets at each instance, appears more and more appealing as an alternative to constructing complex game worlds as it avoids excessive dependence on content design. This is especially true for newer games as there is greater demand for more content in higher fidelity graphics. AAA Titles such as Civilization [23] use seeds in complex models to create different worlds while No Man's Sky [8] iteratively generates entire galaxies, including stars and planets with flora, fauna, and even sentient alien encounters upon discovery.

1.2.   Problem

While procedural generation is not new, it is an exhaustive process which requires consideration of minute details when building the system. AI has been developed for games, such as playing Infinite Super Mario levels [15] but are less proficient when it comes to replicating creative tasks such as level design as the sample space natively adds a greater degree of complexity to the problem. In an attempt to avoid these pitfalls and consume vast amounts of resources for creating multiple levels, exploring deep learning seems to be a favorable course of action. There is a detailed method that is capable of generating DOOM level given certain input criteria through the use of Wasserstein Generative Adversarial Networks (WGAN) [1] with the help of a large repository of custom-made levels created by the community to train the model. While the generation of its level layout is adequate for a First Person Shooter, it is unable to place appropriate game objects into the level layout as it is plagued with disproportionate generation of game object among the present categories and with biased placements, causing them to clump together in certain sections of the level. This results in levels unevenly saturated and biased towards certain types of game objects which hampers the level's ability to properly captivate the player's interest.

1.3. Goals

To improve the DOOM level generator by splitting the problems of planning the level layout and populating it with game objects through the introduction of a hybrid Generative Adversarial Network (GAN) architecture. This requires a repository of DOOM levels that need to be parsed into minimal structures that accurately represent the problematic features. With the feature maps serving as the examples to learn from, the hybrid architecture needs to be trained to learn the different aspects of level design by focusing on patterns present in specific feature maps that are sufficient to design a level until it can reproduce its effects with a degree of efficacy that is both topological and semantically sound. Once the networks accomplish their individual targets, it is compared with the prior design to extrapolate if there are any improvements with the added complexity before being implemented into a level generator. This entails that the generated set of features be reverse engineered into their respective game data to compose the encoded 'lumps' needed to serialize '.WAD' files for the DOOM engine to correctly execute.

1.4. Thesis Structure

The thesis is composed of 6 chapters to compartmentalize the content relevant to this project into their respective sections. This is the 1st chapter which serves as a synopsis of the work that has been put into this thesis. The 2nd chapter showcases a brief overview of relevant research in related fields and suggests the theoretical knowledge required to construct this experiment. The 3rd chapter provides information pertaining to the dataset and its representation that will be used as well as the previous work that has been conducted regarding procedurally generated DOOM. The 4th chapter will deal with how the system is designed and implemented with the format with which the experiments are conducted. The 5th chapter illustrates the results that have been achieved with the designed system with regards to its predecessor through the defined metrics. The 6th chapter provides a summary of the work and preludes possible improvements that can be included in futures developments.

2 | Theory and Motivation

This chapter begins with a brief summary of works that are related to the topic of interest and a dive into the cutting edge of deep learning. This is followed by a review on past methods that have been researched and used for procedurally generating game levels. Finally, an introduction is provided regarding the theoretical foundations required to implement the techniques used in this thesis as well as an explanation outlining how they function.

2.1. Related Works

Artificial Intelligence in Video Games for the most part has referred to the behavior of non-playable characters, but it has been used for much more such as simulating the player or controlling in game systems [16, 21]. The Mario AI competitions [15] saw the mainstream adoption of reinforcement learning (RL) towards simulating the players behavior with similar models outperforming human players in DOOM while also being able to navigate unknown maps [19]. On the other hand, Convolutional Neural Networks (CNN) have been used to predict the outcomes of First Person Shooter (FPS) games to determine if the levels are biased towards a team by its maps and weapon parameters and modifies game data such as character stats and the level layout to control the flow of the game [16].

Through games, AIs have also been taught in real world activities such as the city planner proposed by using RL fractal networks to train agents to maximize the city population in the game SimCity which is further generalized to larger maps using a CNNs with structured skip connections [5]. Mapping and texture design has also been a widely researched field with one such proposal a two-stage GAN framework in which height maps can be randomly generated as well as infer texture maps from the data provided by the NASA 'Visible Earth' project [2]. Its architecture consists of a Deep Convolutional GAN (DCGAN) which generates height maps with a Conditional Generative Adversarial Network (cGAN) for image to-image translation to produce the textures.

2.2. State of the Art

Deep learning has come a long way since the inception of the perceptron in 1943 by Mc-Culloch and Pitt [22]. There have been several architectural leaps that have provided it the maneuverability to permeate into a variety of problems that span multiple fields. This has never been more apparent then during the current resurgence following the pioneering of new techniques like transformers [38] that embed context into sparse representations of text to create 'Chat-GPT' and 'BERT', chatbots capable of conversations indistinguishable from humans on almost any topic. This comes after Recurrent Neural Networks such as the Long-Short Term Memory (LSTM) architecture [13] featured in language modeling and speech recognition until just a few years ago. These found it computationally infeasible to use large contexts from previous outputs, making subpar time-series predictions [43] that pale in comparison.

Larger strides have been made in the domain of images with GANs pioneering its own subset of image generative models such as the Cycle GAN [44], Projected GAN [30] and the Style GAN [17] among others, that have produced realistic visual data of buildings, terrain and textures [2, 37] as well as perform more precise tasks of modifying aspects of images to obtain specific results. Recent advances set forth by the advent of Diffusion Models have brought about systems such as 'DALL-E' and 'Stable Diffusion' that can capture patterns through sequentially denoising autoencoders [27], producing images using text-based cues at a quality never seen before. These have been used from reconstruction of medical images to the restoration and inpainting of video segments to reconstruct missing or damaged regions in an image. It has also been used generate future frames by predicting through an inverse diffusion process [42].

These improvements have also been seen in the fields of computer vision with YOLO models in 2D and 3D detection while graph based methods in the predictions of drug interactions at a level that can more directly impact practical applications. This is seen with the unified representation introduced by YOLOR [39] which has empowered system by including implicit knowledge that serve various tasks, allowing models to learn multiple tasks such as object detection, multi-class labeling and feature embedding all at once. Graph based models such as DSN-DDI [20] have proven its ability to predict interactions from unseen drugs while also being able to combine drugs effectively by means of a dual view representation that performs consistently and can serve as a generalized framework for the discovery of novel drugs and alleviate resources wasted on unproductive clinical trials.

2.3. Literature Review on Procedural Generation of Game Levels

Hendrikx et al. provides a historical survey of methods that have been used for procedural generating for a variety of content in games, including isolated levels [12]. Some of the earlier games surveyed include NPPAngband, an Angband variant, which introduces fractal-based algorithms such as cellular automata for generating caves imitating indoor level design. Many of these algorithms consisted of generative grammars or pseudo random number generator combined with an advanced parameter space search such as a genetic algorithm, often relying on a grid-based structures to generate these levels. Togelius et al. defines a taxonomy using evolutionary/stochastic based optimization algorithms and provides guidelines on how to approach the problem of representation and evaluation [34].

A personalized level generator was proposed by Summerville et al. using an LSTM architecture to classify training levels based on player paths extracted from video clips of them play [32]. The labeled structures serve as input to an auto-encoder which manufactures instances based on the learned design pattern. A similar architecture is used for rhythm-based games by Dance Dance Gradation to invent new levels with different degrees of difficulty with acoustic features obtained from the audio track using a CNN [36]. Another approach that has been taken is training the agents by modeling content generation as a Markov Decision Process to design levels of Zelda and Sokoban using various representations based on the autonomy the agent is given [18].

Park et al. generate levels with a tile-based system for 'Engage', an educational game that helps students learn computer science concepts and practices [24]. It uses a single encoded grid to represent the level layout and multi-step DCGANs to construct solvable levels. One performs training augmentation which creates more training data while another focuses on enhancing solvability by generating levels with higher solvability compared to those concocted by the former. Produced levels are judged using a shortest path algorithm for solvability and a tile comparison through k-nearest neighbors for novelty. It also introduces the concept of variable difficulty to the generator in its level design by classifying levels based on the degree of gaming skill needed to solve the level and its learning objectives to provide a personalized learning experience adapted to each individual player

2.4.   Theoretical Background

2.4.1.   Generative Adversarial Networks

GAN is a framework in which two neural networks are trained simultaneously in an adversarial setting. Generator 'G' generates some target data during the training process while the Discriminator 'D' helps it recover the data generating distribution. This works as a two-player min-max game [10] where the discriminator trains to classify whether the data 'x' is from the real distribution 'p_{data}' or not while the generator uses this feedback for the data it produces with noise 'z' and trains to minimize the discriminator's ability to differentiate it from the real samples.

$$\min_{\{G\}} \max_{\{D\}} \mathbb{E}_{x \sim p_{data}(x)}[logD(x)] + \mathbb{E}_{z \sim p_z(z)}[log(1 - D(G(z)))] \qquad (2.1)$$

The two networks are trained simultaneously through gradient descent performed over the loss which is calculated iteratively and is back-propagated over to the network's weights and biases until a local minimum is achieved. This is done by estimating lower-order moments '$\hat{m}$' and '$\hat{v}$' via an Adam optimizer that uses stochastic gradient descent with 'α' as the step size and 'θ_0' being the initial parameter vector of the network.

$$\theta_t \leftarrow \theta_{t-1} - \alpha \cdot \hat{m}_t/(\sqrt{\hat{v}_t} + \epsilon) \qquad (2.2)$$

Figure 2.1: Generated results using the MINST and TFD dataset from the work of Goodfellow et al.

2.4.2.   Deep Convolution Generative Adversarial Networks

To overcome the difficulties of modifying GANs using the CNN architecture to work with images, DCGANs removes fully connected hidden layers for fractional-strided convolutions in the generator and strided convolutions in the discriminator [25]. This essentially swaps the optimization problem into learning an effective kernel that is able to generate the desired distribution. Spatial pooling functions are replaced since global average pooling increases model stability at the cost of convergence speed. To optimize this trade off, the convolutional features are directly connected to the input and output layer of both the networks. After each convolutional layer, Leaky Rectified Linear Unit (Leaky ReLU) activation functions are used in the generator and discriminator as it allows for back-propagation even for negative input values except for the output layer of the generator, which uses the Tanh function to quickly learn to saturate the color space for the training distribution completely.

Figure 2.2: Generated bedrooms using the LSUN dataset after five epochs of training from the work of Radford et al.

2.4.3.   Wasserstien Generative Adversarial Networks with Gradient Penalty

As DCGANs use a Binary Cross Entropy Loss function instead of the KL divergence to minimize the Jensen Shannon divergence in GANs, they suffer from the generator's tendency to converge towards a singular solution to fool the discriminator (mode collapse) and vanishing gradients of discriminator predictions when trained to optimality. This is potentially from the generator's parameter space not being continuous and is addressed by using Wasserstein-1 distance to expresses the dissimilarity between two distributions through the minimum cost to rearrange to one distribution to another [1]. This Wasserstien GAN (WGAN) reconstructs the min-max game using the Kantorovich-Rubinstein duality with sample $\tilde{x}$' belonging to the generated distribution $\mathbb{P}_g$' and 'x' to the real distribution '$\mathbb{P}_r$'.

$$\min_G \max_{D \in \mathcal{D}} \mathbb{E}_{x \sim \mathbb{P}_r} [D(x)] - \mathbb{E}_{\tilde{x} \sim \mathbb{P}_g} [D(\tilde{x})] \tag{2.3}$$

Another variation added to the traditional WGAN consists of a more robust loss function that accounts for higher order moments of the data distribution by introducing a penalty on the gradient norm for random samples '$\hat{x}$'. Unlike the k-Lipshitz constraint previously implemented through weight clipping, that biases the critic towards simpler functions, this gradient penalty enforces a 1-Lipshitz constraint on the gradient norm of the critic's output to its input [11].

$$L = \mathbb{E}_{\tilde{x} \sim \mathbb{P}_g} [D(\tilde{x})] - \mathbb{E}_{x \sim \mathbb{P}_r} [D(x)] + \lambda \mathbb{E}_{\tilde{x} \sim \mathbb{P}_{\tilde{x}}} [(\|\nabla_{\tilde{x}} D(\tilde{x})\|_2 - 1)^2] \tag{2.4}$$

Traditionally, DCGANs normalizes each feature independently across the batch to prevent the generator from collapsing all samples to a single point before every layer (except the generator's output layer and critic's input layer as it results in sample oscillation and model instability) but doing this changes the problem from individual mapping to mapping the entire batch for the discriminator. Thus, batch normalization is substituted with layer normalization in the critic since it does not introduce correlations between examples and the penalized training objective is now calculated using the norm of the critic's gradient with respect to each input independently.

2.4.4.   U-Net

A classification network consisting of contracting layers to capture context and symmetrically expanding layers that enables localization [28]. The contracting path iteratively applies unpadded convolutions with rectified linear unit activations and max pooling operations for down sampling. The expansive path up samples and performs transposed convolutions, concatenated with the corresponding features from the contracting path and is followed by a convolution and rectified linear unit (ReLU) activation at each iteration.

$$p_k(x) = exp(a_k(x))/(\sum_{k'=1}^{K} exp(a_{k'}(x))) \tag{2.5}$$

The network's loss is computed with a pixel-wise soft-max through the use of a cross-entropy loss function. The activation 'a_k' for the set of classes 'K' at the pixel position 'x' is used to approximate a maximum function '$p_k(x)$' that is meant to identify the true class for the image by bringing the results of the class with the maximum activation closer to 1 while dropping the output for the remainder of the classes near to 0.

$$E = \sum_{x \in \omega} w(x) log(p_{\ell(x)}(x)) \tag{2.6}$$

The cross entropy then penalizes at each position the deviation of the activation '$p_{\ell(x)}$' from the true label 'ℓ' for each pixel and uses a pre-computed weight map 'w' to give more importance to certain pixels while the network is training and compensate for the different frequency of pixels in the training dataset. Their initial weights drawn from a Gaussian distribution such that features has approximately unit variance and optimized through minimizing the Euclidean distance by averaging all plausible outputs with high momentum to ensure that the current optimization step is based more on previously seen training samples.

2.4.5.   Conditional Generative Adversarial Networks

Unlike conventional GANs, cGANs use a "U-Net"-based architecture as its generator to perform image-to-image translations by mapping input images 'x' towards the desired output images 'y' using the noise 'z'. It employs an $L1$ loss that can accurately capture the low frequencies but produces blurry results since it cannot capture high frequency crispness. Thus, a Patch classifier is also incorporated which only penalizes structure at

the scale of image patches to model high frequency structures.

$$L_{L1}(G) = \mathop{\mathbb{E}}_{x,y,z}[\|y - G(x,z)\|_1] \tag{2.7}$$

$$L_{cGAN}(G, D) = \mathop{\mathbb{E}}_{y}[log D(x,y)] + \mathop{\mathbb{E}}_{x,z}[log(1 - D(x, G(x,z)))] \tag{2.8}$$

This tackles the issues of blurriness by classifying patches of an image as real or generated by running it convolutionally across the image, assuming independence between pixels separated by more than a set patch diameter and averaging all responses [14]. The objective is realized as a min-max game with an additional $L1$ loss that is amplified through 'λ'

$$\min_{G} \max_{D} L_{cGAN}(G, D) + \lambda L_{L1}(G) \tag{2.9}$$

As such a network requires low-level information shared between the input and output, it uses small batches with high momentum while retaining batch normalization and dropout.

Figure 2.3: Generated results on Satellite and translated images from Google Maps from the work of Isola et al.

3 | Representation and Prior Design

3.1. DOOM

In this thesis, the experiments are built around the game Doom (1993) published by id Software. It was pivotal in the establishment of the genre now known as First Person Shooters, putting forward a novel technique for 3D graphics as well as initiating support for custom modifications in its level format through its ports. As one of the earliest 3D games, DOOM is viable subject as it has many freely accessible custom levels that has been developed by the community which is tracked by websites such as 'Doomworld'. It also benefits from its simpler 2D representation despite its 3D player environment, drastic simplifying its representation and subsequently reducing the computational costs due to the reduced sample space, with widely available documentations allowing for it to be easily parse. It spawned dozens of 'DOOM Clones' with Figure 3.1 showing that more than half the code base is cloned in certain older titles [4].
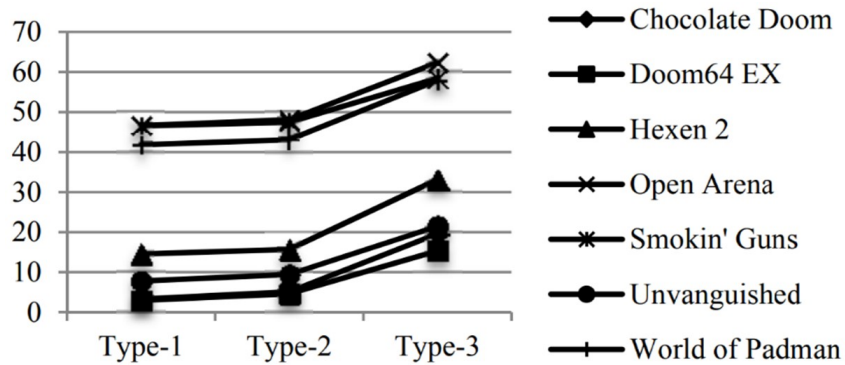
Figure 3.1: Percentage of Total Cloned Lines of Code with exact code clones (Type-1), similar code fragment with only different token names (Type-2) and similar algorithms (Type-3) from the work of Chen et al.

3.2.   WAD

3.2.1.   Format

Levels in DOOM are stored in '.WAD' format and contain all the necessary information for the DOOM engine to create the level [6]. The game was sold with 9 official levels which are Internal WADs or IWADs. These explicitly define each of the features such as terrain and game objects as well as any graphics and sound required by the level. The dataset used in this experiment are solely Patch WADs or PWADs which are levels built by the community through map editors such as DOOM Builder. They contain custom content or modifications that either add to or replace those already present in the original IWADs.

3.2.2.   Structure

Each WAD is composed of byte data ordered as a sequence of lumps which is used by the DOOM Engine to build the level. It is preceded by a header that provides the WAD's metadata and is succeeded by a directory containing metadata on every lump.

Section Length (bytes)	Section Name	Field Size (bytes)	Field Name	Description
12	Header	4	Identification	'PWAD' or 'IWAD' in ASCII
		4	Number of Lumps	Integer value of lumps included in WAD
		4	Table Offset	Integer pointer to resource dictionary
Variable	Lumps	-	Lump Data	Lumps stored as a byte stream
16 * Number of Lumps	Directory	4	Lump Position	Pointer to respective lump data
		4	Lump Size	Size of respective lump in bytes
		8	Lump Name	Lump Name in ASCII

Table 3.1: Sections of a WAD as seen in the work of Giacomello et al.

3.2.3.   Contents

All the information about the DOOM level that is used by its engine can be found within
their respective lumps with each designated to a specific component of the level structure.
The lumps defined in the Table 3.2 and Table 3.3 represent the mandatory set of lumps
necessary for any WAD to be accepted as an admissible DOOM level. Most entries in the
lumps are separately partitioned into a set of fields. Multiple entries in different lumps are
used to define entities and provide the needed metadata to signify special effects through
fields allotted to flags which are present in all unique lumps except for name and vertexes.

Lump Name	Description	Entry Size (bytes)	No. of Fields
NAME	The IWAD level name either as an 'ExMy'label where 'x' is the episode number and 'y' is the mission number for DOOM or an 'MAPzz' label with 'zz' as the level numberfor DOOM 2 in ASCII	2	1
THINGS	A list of game objects in the level that is not a wall, pavement or door with its position and orientation identified using an index	10	5
LINEDEFS	A list of every line needed to signify all the walls, steps, and invisible boundaries such as triggers for events that shape the level	14	7
SIDEDEFS	A list of textures referenced by the LINEDEF for either side. It also specifies the sector number that this plane is facing, implicitly defining the sector boundaries	30	6
VERTEXES	A list of x and y map coordinates that are referenced by LINEDEFS to create shapes on the map	4	2
SECTORS	A list of closed areas with the same textures as well as floor and ceiling height. Additional fields describe its lighting and the floor's special effects that usually damage the player	26	7

Table 3.2: Unique mandatory lumps in a WAD

The level building process begins through the designation of an individual sector and iterative laying out its components until all the sectors are rendered. Sectors are constructed using the relevant linedefs that are obtained through the sidedefs that reference the respective sector. Linedefs are defined using two entries from the vertex lump and can mention only a right sidedef for boundary walls. When connecting two sectors, linedefs will mention both sidedefs and can act as triggers using the corresponding flag. There are also certain constraints to the formation lumps used to define a level such as the presence of exactly one 'NAME' lump in every WAD and the inability to render sectors above or below another since it uses a 2D map. Other functional lumps can be derived from the former using 3rd party software and serve to speed up the rendering process by avoiding runtime computation. All the lumps mentioned here except REJECT are mandatory for the engine to be able to build the level. These include:

Lump Name	Description	Entry Size (bytes)	No. of Fields
SEGS	A list of wall segments comprising either a part or all of a LINEDEF which are combined to form the various sub-sectors	12	6
SSECTORS	A list of sub-sectors which are the smallest undivided spaces incapable of obstructing the visibility of other walls within it	4	2
NODES	Branches in a 2D binary space partition tree sorting the view order of each sub-sector which speeds up the rendering process	28	8
BLOCKMAP	Pre-computed collision detection mapwithout which objects and walls within the level cannot interact with any another	-	-
REJECT	Table to determining if an agent can ascertain the players location for isibility calculations which are used to optimize the AI routines	1	8

Table 3.3: Derivable mandatory lumps in a WAD

These lumps speed up the rendering process by using a graph to represent the overall structure of the level and decide what needs to be shown by taking into account the player position and sorting the sub-sectors that are supposed to be visible to user. This is achieved by using the sub-sectors composed of segments as nodes in the graph that are rearranged every time the player moves through partition lines that divide the map and get progressively smaller for each child until all sub-sections have been encompassed.

Some of the derivable lumps have more unique structures such as the reject which expects byte sized entries with each bit representing visibility from a sector and the final byte padded to meet the size requirement. The blockmap on the other hand is preceded by a header of 8 bytes indicating the coordinates of the origin and the number of blocks within the grid, after which the offset of the linedefs is provided and is followed the line segment.
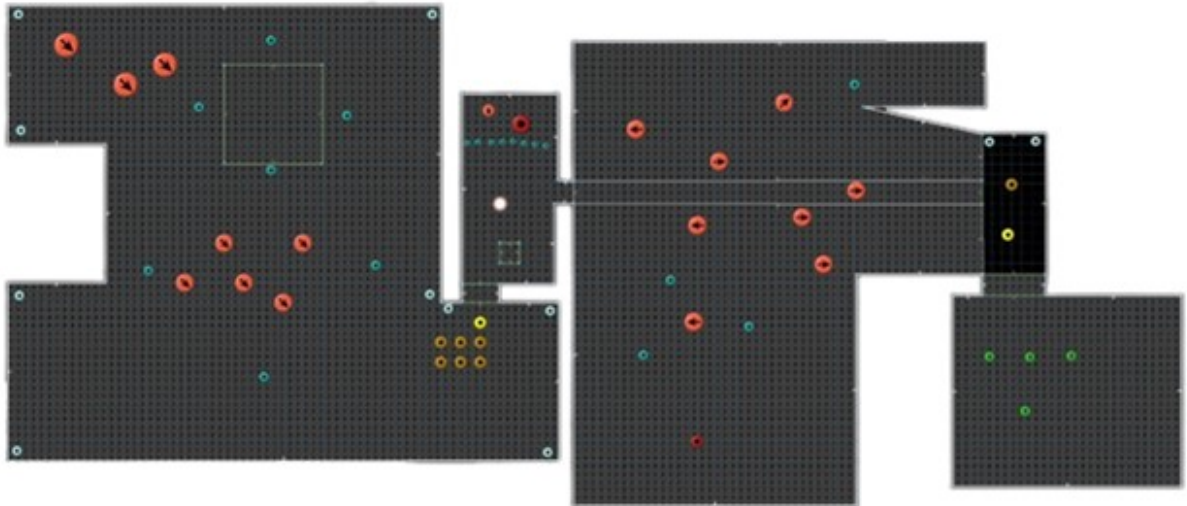
Figure 3.2: Sample DOOM PWAD visualized using DOOM Builder where orange indicates enemy positions, yellow represents pick-ups such as power-ups/ammunition and green is the starting position of the players

3.3.   Giacomello's DOOM Level Generator

3.3.1.   Dataset Organization and Presentation

WADs are converted into feature maps which function as the training data for the neural network. This is done by translating extracted byte data by means of a custom parser and composing them into local data structures for the aforementioned lumps. By focusing on the minimum requirements necessary for creating a DOOM level, the parsed dataset is limited to 4 feature maps which represent the level topology as well as its functional components. To this end, the wall, floor, and its height proved capable of accurately representing the level layout while the things map handles the presence of gameplay elements. After parsing the WAD, relevant coordinates for each map are marked on separate matrices. The dimensions of this matrix are allocated based on the length and width of the given map, scaled down from its original size by the radius of the smallest function object, in this case by 32 times.

The level shape is sketched out via sectors through finding all sidedefs with the same number in the sector field and obtaining all the linedefs that reference these sidedefs. The retrieved list of linedefs is used to identify the pertinent vertices which are then adjusted for the new scale of the map. The wall map is outlined by drawing lines between the referred vertices for each linedef only if it contains at least one sidedef that is not transparent. The height map is computed sector wise by extrapolating the perimeter given by these lines and iteratively traces out the respective polygons that envelope the area containing that sector. The floor map is obtained by creating a mask of the positive value in the height map while the things map uses the scaled coordinates to encode pixels with values from the things type dictionary.

A further set of scalar features such as the ratio between the level area and its convex hull, mean room size, largest room size, room count, diameter of circle with the same level area, length of the longest and shortest axis of the level as well as the skewness and peak sharpness in the pixel distance distribution from its closest wall are also computed and appended to the maps as part of the dataset. This is done in order to provide some degree of control over the generation process as they are easily extracted and impervious to noise. The dataset is then stored as Tensorflow records to avoid recalculation.

Figure 3.3: Floor map, Height map, Wall map, and Things map (from left to right) of a sample level

The feature maps shown in Figure 3.3 represent the level in its bare minimum and are used to derive all the mandatory lumps required to furnish a level while delivering the gameplay envisaged by the genre. The features maps are engineered as such:

- FLOOR MAP: Depicts the floor layout of the level by segregating the available space into the portion that lies within bounds of the level using pixel values of 255 to denote them and leaves that which remain with a pixel value of 0.

- HEIGHT MAP: Marks the height of various sections of the map by encoding pixel values in gradients for segregating each sector with a maximum value of 255 and those outside the bounds of the floor map as 0.

- WALL MAP: Compartmentalizes the level into separate rooms and visualizes the points of access for each of the rooms by tracing the positions of the walls used to partition it. Walls are marked with a pixel value of 255 while the rest are left with a pixel value of 0.

- THINGS MAP: Indicates the position of the game objects on the map by identifying the type of object through pixel values assigned using the id allotted to it in the things type dictionary while the absence of objects is represented as 0.

3.3.2. System Architecture

Giacomello approaches the problem of procedurally generating DOOM levels by means of a Conditional Wassertien GAN with a Gradient Penalty [9]. By rescaling the feature maps extracted from the TFrecords into the same shape of 128 by 128 pixels, the generator is trained on a normalized version of the dataset which is further enlarged by including three more orientations by rotating the maps in multiples of 90-degree. The extracted input scalars called 'Feature Vectors' are also appended to the feature maps to control the generation process to some extent.

Figure 3.4: Conditional GAN architecture used for the generation DOOM levels from the work of Giacomello et al.

The generative network has five hidden layers which comprise of one linear layer followed by convolutional layers with a final convolutional output layer applying a sigmoid activation function as it better coincides with the target format. It uses the feature vectors accompanied by a gaussian noise vector as input and learns its distribution while the critic uses the real feature maps and the generated ones grasp the differences between them given those feature vectors. The model's predictions are then evaluated based on the Wasserstien distance from its expected value. The parameters are then adjusted using an Adam Optimizer with the generated levels compared using metrics such as corner count, structural similarity index and encoding error to assess the quality of the developed architecture.

3.3.3. WAD Generation

Once the network is capable of generating maps recognizable as DOOM levels, a custom WAD writer is used to reverse engineer the matrices into lumps of byte data representing the mandatory components of a PWAD. By using the floor, wall, height, and things feature maps, it prepares the level layout by reconstructing the information into an undirected weighted graph. This is done through computing the respective room maps by means of a segmentation algorithm to compartmentalize sections of the walkable area of the level. The graph is then constructed outwards from the center and is decorated with various features while keeping the textures constant.

Level paths that can be traversed are collected using a minimum spanning trees algorithm on the graph from the section of the level with the least entrances which is used as the starting position of the level. Based on the computed solutions, an exit trigger is generated at the end of the longest floor path. Once the graph is complete, its nodes are translated into their respective lumps by scaling up each of the coordinates by 64 before it is finally committed with a level name and generated as a WAD. Four texture entries are required in all such PWADs for DOOM to run properly which are '$FLOOR4_8$', '$SFLR6_1$', '$MFLR8_4$', and '$FLOOR7_2$'. The first three are needed as backgrounds for the episode end texts. The last is what is shown outside the border of the display window when not being run in full screen.

3.3.4. Drawbacks

Due to the use of interpolation techniques to resize the image into identical shapes, the information within the images is not exactly translated when performing such transformations. Effects of distortion and blurring can be addressed or ignored during the dataset preparation for the topological maps as the variation is consistent in the height map while the floor and wall maps are indifferent to exact pixel values. Sparse images such as the things map depend on the pixel encoded values which are contorted beyond the permissible levels of tolerance, making it to be difficult to maintain its integrity. In the case of the things map, this has the effect of pixels taking on the value of other objects, coercing them towards objects with lower assigned ids. Multiple objects close together also get overlooked when larger maps are scaled down from their original size based on the order the object is presented with the WAD. This is due to compacting the level space which results in large units of area converging into a single pixel and the indiscriminate superseding by the last object in the list regardless of category, further dissociating the relations between object types.
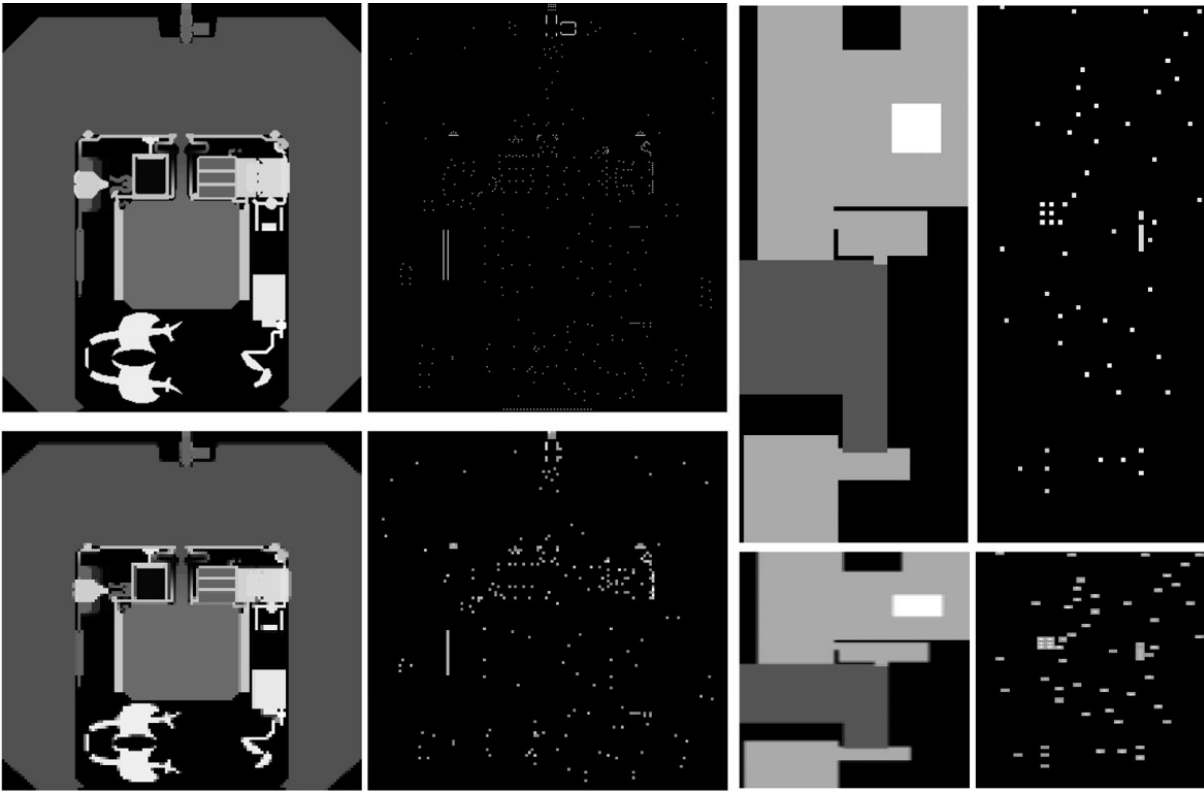
Figure 3.5: Height and Things maps (From left to right) of the sample levels (above) compared to its resized counterpart (below)

Maps smaller than the target size of 128 by 128 pixels on the other hand must be enlarged to compensate for the lack of area which leads to objects being represented through the multiple surrounding pixels, further deteriorating the quality of the map. It also leads to large empty spaces throughout the level which can throw of the networks ability to learn and populate the level space completely.

There are bugs encountered in the generation process as disconnected sections of the level are inaccessible and the objects present within these portions of the level do not meaningfully contribute in any way to the actual proportions of the category types. If the player spawns in a section that has a greater population of monsters while another detached section has more ammunition, it presents the player with little to no opportunity to exploit the totality of resources available. Attached segments can also be inaccessible when the connecting corridors are too small to traverse, only allowing the player to peek through which is detrimental to gameplay.

3.4. Improved Feature Map Extraction

To alleviate some of the problems encountered, modifications have been made to Giacomello's WAD Editor to parse the WADs for a better representation of the sufficient subset of unique feature used to design a level. From Figure 3.6, it can be noted that most maps lie below 15000 units in both dimensions from the figure. The parsed maps are now scaled down to 256 by 256 pixels with levels below 15000 units being relatively padded by two row or columns for every 300 units smaller than the mentioned limit in its respective dimension to preserve objects density. Although there is still some overlap among game objects, integrity of pixel values is ensured by using only coordinate rescaling instead of resizing throughout the entire process.
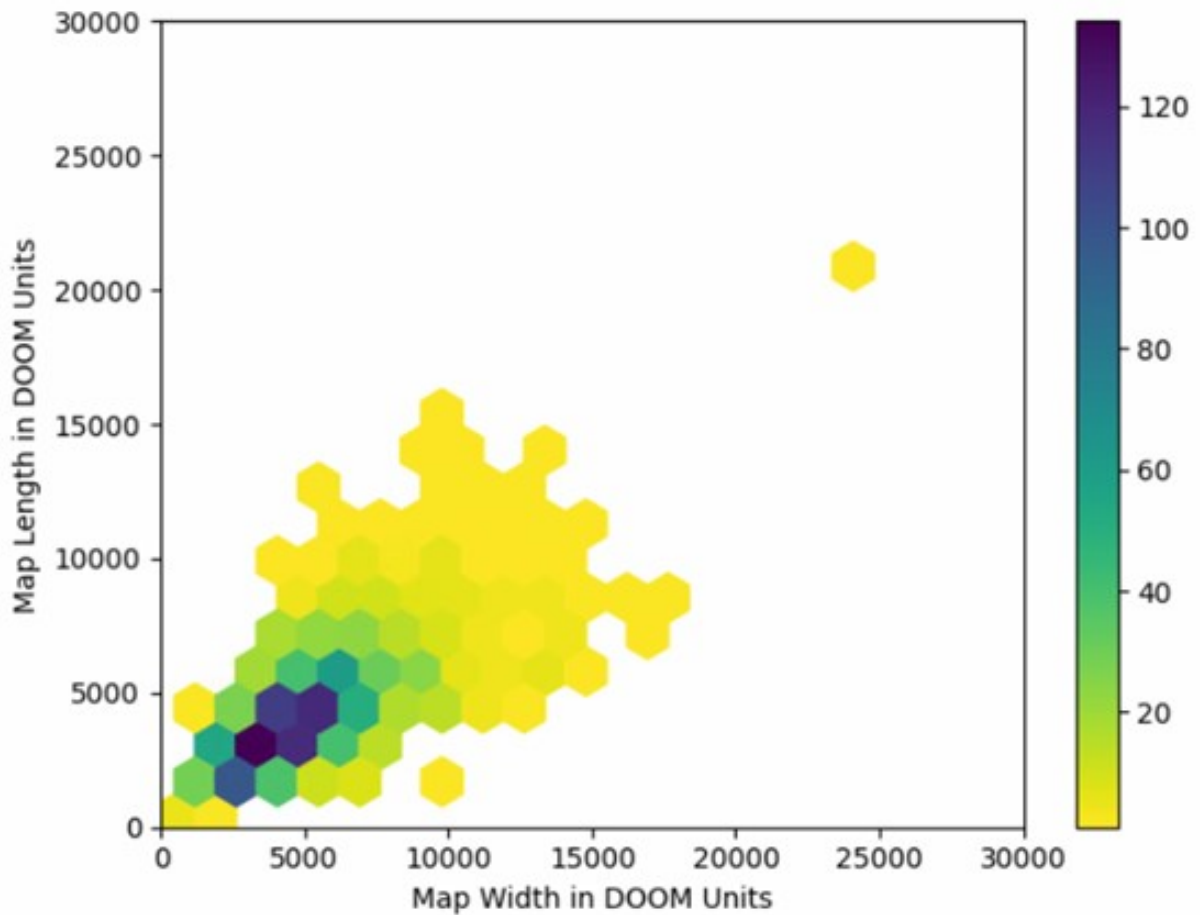
Figure 3.6: Area distribution of the filtered dataset

While retaining the topological maps, the things map has been further divided into their individual category maps to provide a more coherent context for the system to process. Objects of the respective category are designated an id, acquired by arranging them in

the order of significance of the effect it has on gameplay. Only functional elements that are required to fully experience the game have been factored in and can be recombined to recreate the thingsmap. The categories included are monsters, ammunition, power-ups, artifacts, and weapons.
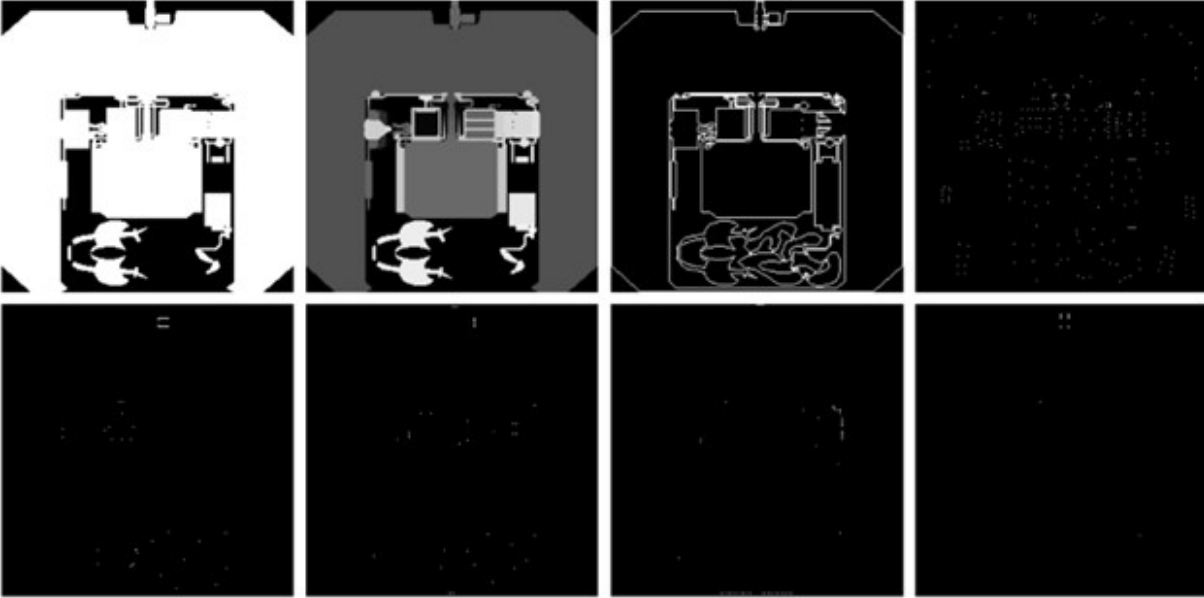
Figure 3.7: Floor, Height, Wall, Monsters, Ammunition, Powerups, Artifacts and Weapons map (From left to right, top to bottom) of the sample level using coordinate rescaling

The newly added set of feature maps apart from the included floor, height and wall maps from the previous design are:

- MONSTERS MAP: Assigns the respective positions of enemies with the pixel value corresponding to its monster id and 0 representing its absence.

- AMMUNITIONS MAP: Assigns the respective positions of munitions used by the various weapons with the pixel value corresponding to its ammunition id and 0 representing its absence.

- POWERUPS MAP: Assigns the respective positions of armor and first aid with the pixel value corresponding to its powerup id and 0 representing its absence.

- ARTIFACTS MAP: Assigns the respective positions of specialized abilities with the pixel value corresponding to its artifact id and 0 representing its absence.

- WEAPONS MAP: Assigns the respective positions of the various weapons with the pixel value corresponding to its weapon id and 0 representing its absence.

Mentioned in Table 3.4 and Table 3.5 are the list of game objects that have been taken into consideration as they provide a functional value to the setting of the game. Apart from the start position of the player, the remainder of the objects are generated using the implemented model.

Id	Things Type Id	Description	Category	Category Id
1	0	Empty	-	0
2	3	Player 1 Start	other	1
3	75	Arachnotron	monster	11
4	76	Arch-Vile	monster	14
5	77	Baron of Hell	monster	16
6	78	Cacodemon	monster	9
7	79	Chaingunner	monster	7
8	81	Cyberdemon	monster	17
9	82	Demon	monster	4
10	83	Former Human Trooper	monster	3
11	84	Former Human Sergeant	monster	5
12	85	Hell Knight	monster	15
13	86	Imp	monster	1
14	87	Lost Soul	monster	8
15	88	Mancubus	monster	13
16	89	Pain Elemental	monster	10
17	90	Revenant	monster	12
18	91	Spectre	monster	6
19	92	Spider Mastermind	monster	18
20	93	Wolfenstein SS	monster	2
21	94	Ammo Clip	ammunitions	2
22	95	Box of ammo	ammunitions	6
23	96	Box of rockets	ammunitions	7
24	97	Box of shells	ammunitions	5
25	98	Cell charge	ammunitions	4

Table 3.4: List of relevant game objects with category ids (1 of 2)

Id	Things Type Id	Description	Category	Category Id
25	98	Cell charge	ammunitions	4
26	99	Cell charge pack	ammunitions	8
27	100	Rocket	ammunitions	3
28	101	Shotgun shells	ammunitions	1
29	102	BFG9000	weapons	7
30	103	Chaingun	weapons	3
31	104	Chainsaw	weapons	1
32	105	Plasma Rifle	weapons	6
33	106	Rocket Launcher	weapons	5
34	107	Shotgun	weapons	2
35	108	Super shotgun	weapons	4
36	109	Backpack	powerups	3
37	110	Blue armor	powerups	5
38	111	Green armor	powerups	2
39	112	Medikit	powerups	4
40	113	Radiation suit	powerups	6
41	114	Stimpack	powerups	1
42	115	Berserk	artifacts	3
43	116	Computer map	artifacts	5
44	117	Health potion	artifacts	1
45	118	Invisibility	artifacts	8
46	119	Invulnerability	artifacts	9
47	120	Light amplification visor	artifacts	7
48	121	Megasphere	artifacts	6
49	122	Soul sphere	artifacts	4
50	123	Spiritual armor	artifacts	2

Table 3.5: List of relevant game objects with category ids (2 of 2)

4 | Implementation

4.1. Dataset Procurement

The data used to train and validate the models is obtained by scraping custom made doom levels from Doomworld.com, a source mirror of Idgames Archive. A scraper is made to access the domain and iterates over the webpages of the available levels within each subcategory present excluding 'Deathmatch', 'Megawads' and 'Ports'. This choice has been made to avoid mixing different types of levels as player vs player environments are structurally different from player vs enemy environments. Ports has been ignored because it requires modifying the game engine to run the level which is complicated to characterize in a format decipherable by the model and stably implement into PWADs. The web scraper then downloads WADs and stores the relevant information in a JSON file which doubles as register to catalogue the collection at hand.

Among the custom levels present in Doomworld's repository, 1969 of the available levels do not fall within the excluded categories mentioned above. In an effort to reduce the complexity of the problem, WADs containing only a single level have been included to ease the requirements of the system with a simpler manner of representation. Similarly, constraints have been placed on the levels to ensure its faithfulness to the genre is respected such as accepting only those that contain at least one monster and weapon to improve the overall consistency within the dataset. Finally, to forgo the intricacies that arises with teleporters, levels that have large, detached segments have not been included leaving only the remaining 1089 levels which are taken into consideration and included in the finalized dataset. The WADs that have been determined to meet the desired criteria are then parsed and have its feature maps extracted to serve as the training data for the models.

4.2.   System Architecture
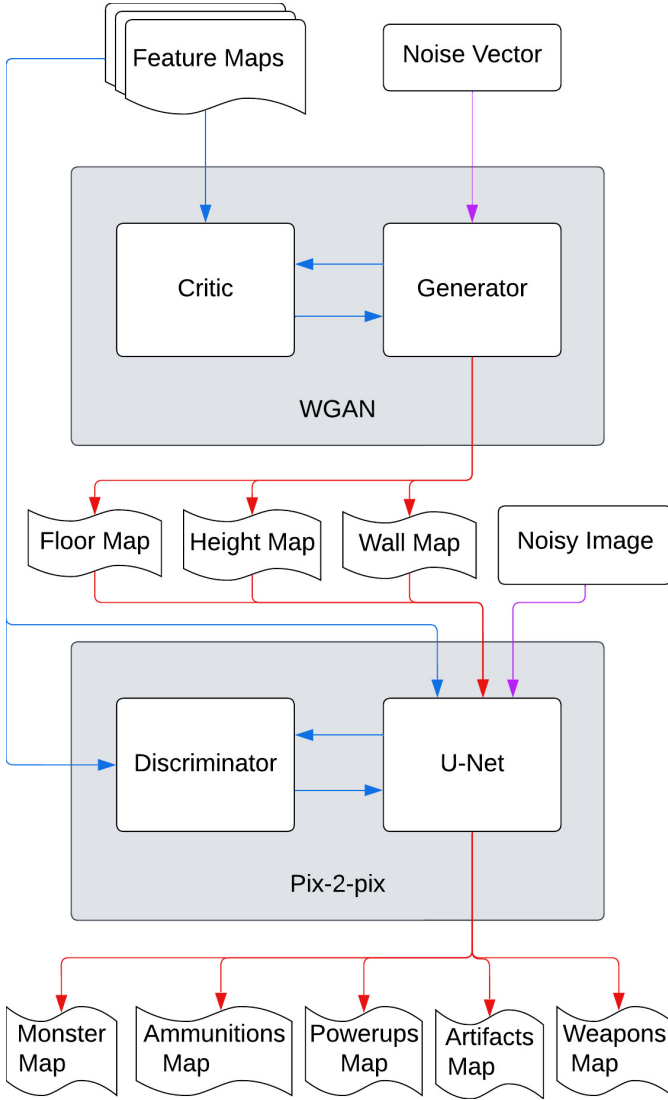
Figure 4.1: The hybrid GAN architecture where blue lines represent the training process, red line are used in the generation process and the purple lines are for both

The proposed system is a hybrid architecture consisting of a WGAN-GP and a cGAN model that are trained on specific feature maps to grasp particular aspects of level design. The WGAN-GP is provided with those pertaining to the level's topology to learn to draft coherent level layouts while the cGAN is taught the functional aspects of the level that it uses to spawn game objects in a manner that positively influences the game dynamics within the generated level. These networks are built using the Keras Sequential API from the Tensorflow libraries in Python 3.9.

The models are split into individual networks and are trained separately due to the size restriction on the memory of the GPU. During the generation process, the networks are run consecutively with the WGAN-GP executed first so that its results can be fed into the cGAN after certain post processing. The results obtained from both the networks are then concatenated together to attain a complete set of feature maps which are then used to manufacture the mandatory lumps and assembled into

a WAD. The remaining lumps are procured using a 3rd party software and this process is explained in greater detail in the following sections.

4.3.   Network Components

4.3.1.   Topological Generator

The subsystem is designed using Radford and Metz's Deep Convolutional Generative Adversarial Network architecture with Wasserstien distance used to calculate the loss as undertaken by Arjovsky et al. The generator is trained alongside a critic implementing alterations by Gulrajani et al. which incorporates a gradient penalty to its loss estimation and has the inclusion of additional training steps compared to that of the generator. The aim is to teach this module the topological structure of levels which is defined by its floor space, the enclosing wall layout, and the respective height of each section.

The data handled involves a random gaussian noise vector 'Z', the topological feature maps 'X' and the critic's classification of the allocated map 'Y'. The topological feature maps consist of the floormap, wallmap and heightmap images and those obtained from the scraped dataset represents the real distribution 'X_{True}' that the generator is to learn. These are used in combination with images from the generated distribution to help the critic determines which features needs to be extracted to correctly classify a provided image. The sampled feature maps 'X_{Gen}' from the generated distribution is procured using the generator 'G' through manipulation of the noise vector i.e.,

$$X_{Gen} = G(Z) \tag{4.1}$$
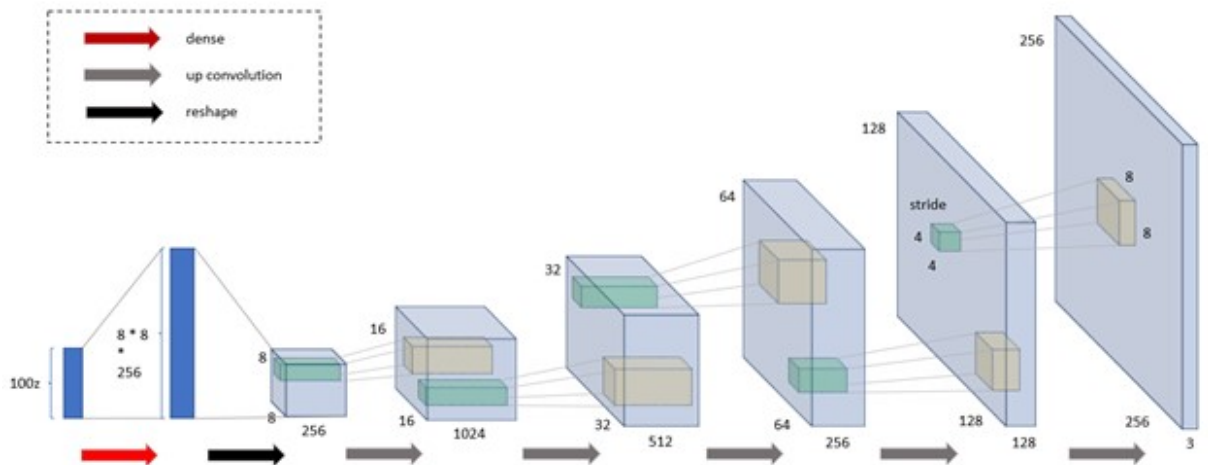
Figure 4.2: Topological generator of the hybrid architecture

It uses an identical architecture to the previous design, taking in a 100-element noise vector as input and manipulating the tensor length through a dense hidden layer to project the noise into a larger tensor. The tensor is then reshaped into a set of 8 by 8 images which are then expanded through a series of up convolutions until the final output layer produces a floor, wall, and height maps for the generated level of size 256 by 256. A sigmoid activation function is used in the output layer instead of the orthodox tanh function as it is more appropriate as the constraint the feature maps lie within the normalized limits.

Similarly, the critic 'C' is constructed in the same manner with the only difference being that it operates on three feature maps. It processes the maps with its hidden layers iteratively through repetitive steps of down convolution followed by layer normalization and Leaky ReLU activation until it is finally condensed into a single output assigning the map belonging either to the real distribution 'Y_{True}' and the generated distribution 'Y_{Gen}' to a value between 0 and 1. It is equivalent to the logits functions where it optimizes the critic's prediction as follows:

- $Y_{Gen} = C(X_{Gen}) = Logits(X_{Gen})$ are brought closer to 0 as it indicates that the sample is generated.

- $Y_{True} = C(X_{True}) = Logits(X_{True})$ are brought closer to 1 which symbolize that the sample is real.

4.3.2. Functional Generator

The module is based on Isola et al.'s Conditional Adversarial Network with modifications made to its loss function to help better extract the target distribution in the given circumstance. The generator's architecture uses the three 256 by 256 pixel topological maps 'X_I' with an image of gaussian noise 'Z' of the same size and progressively transforms the tensors into the category maps 'X_T' consisting of the monsters, ammunition, powerups, artifacts and weapons maps. The network is initially trained to generate category maps 'X_{T_Gen}' using the sample input 'X_{I_True}' from the real distribution. It is then compared with the original object map 'X_{T_True}' by the discriminator. During the generation phase, the network uses the maps 'X_{I_Gen}' produced by the topological generator to obtain the newly generated category maps 'X_{T_GGen}'.

$$X_{T\_Gen} = G(Z|X_{I\_True}) \tag{4.2}$$

$$X_{T\_GGen} = G(Z|X_{I\_Gen}) \tag{4.3}$$

The generator is trained in a method which requires it to retain its batch normalization even after the training process. Instead of using a tanh activation function for the generator output layer, a Rectified Linear Unit activation function has been used as it has proved to provide better image translation. The generator loss function has also been modified to account for the problems parameters and as such it contains the adversarial loss i.e binary cross entropy but has the L1 loss substituted with the sum of the object and mask loss which is explained in greater detail in the next section.

The discriminator classifies the samples from the real distribution much like that of the WGAN with the only difference being its Binary Cross Entropy loss function. Both the generator and discriminator of the conditional adversarial network use modules of the form convolution, followed by batch normalization and a rectified linear unit activation. The predictions are composed as patches which are calculated similar to logits and are optimized as

- $Y_{Gen} = D(X_{I\_True} + X_{T\_Gen}) = Logits(X_{I\_True} + X_{T\_Gen})$ are brought closer to 0 as it indicates that the sample is generated.

- $Y_{True} = D(X_{I\_True} + X_{T\_True}) = Logits(X_{I\_True} + X_{T\_True})$ are brought closer to 1 which symbolize that the sample is real.
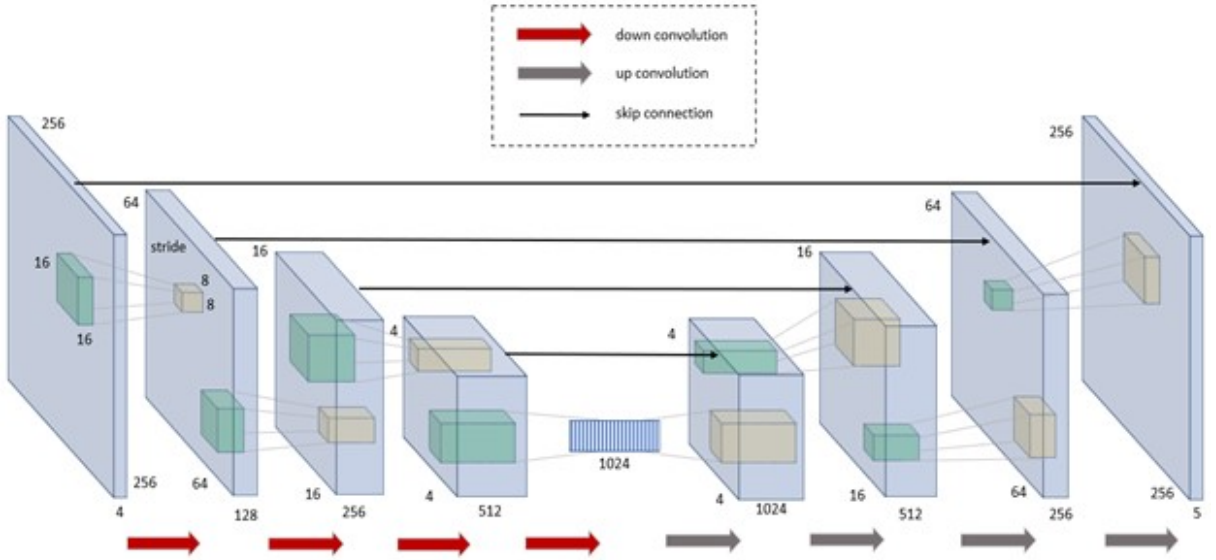
Figure 4.3: Functional generator of the hybrid architecture

4.3.3.   Data Flow
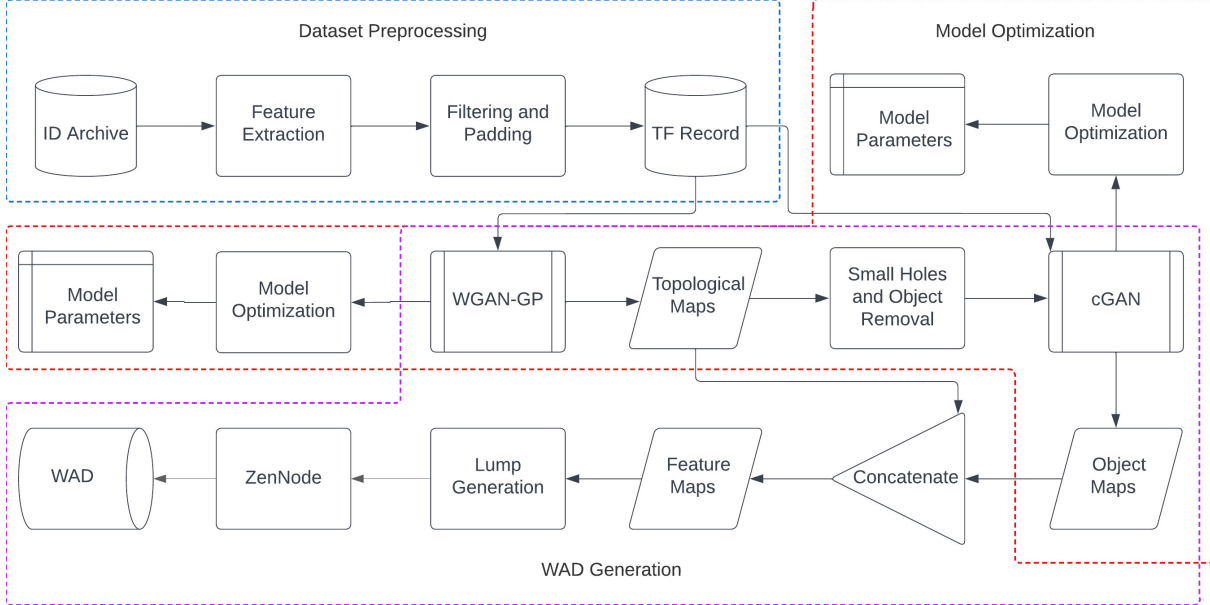
Figure 4.4: Data flow diagram

The flow of data varies between the two use cases that are being performed by the system. The first of which is the dataset processing phase which begins with the dataset procurement of level repository from the archives that appears in the top left of Figure 4.4 to obtain the dataset as TFRecords. Once the dataset is procured, the operation is concluded, the model optimization phase uses the dataset until the constructed models have been sufficiently taught to obtain the feature maps that can mimic the dataset.

The next case is the generation phase, during which the models transform random noise into feature maps with the WGAN's outputs go through a post processing phase to help clear noise and artifacts. The resultant maps are then validated to ensure the absence of anomalies before being supplied to the cGAN. Then the model outputs are tested through evaluation metrics to inform of its quality and converted into WADs for examination of possible in gameplay.

4.4. Model Optimization

4.4.1. Modified Loss Function

While the WGAN uses the loss function defined in Section 2.4.3, the cGAN network faces the same issue when it comes to the sparse nature of the category maps. This is because the mean produces negligible values which prove detrimental in inferring the loss. Thus, a suitable loss function has been hand crafted for the problem which moves away from the $L1$ loss by replacing it with more appropriate metrics. The first of which is the mask loss 'L_M' which is used to compute the number of objects that deviate from the bounds of the level.

$$L_M = ln|1 + \sum_{i=0}^{n} b_i \cdot B(X_{T\_Gen_i})| \tag{4.4}$$

Where 'b' indicates if pixel 'i' is not within the level bounds through taking the logical not of the floor mask and 'B' is the binary of the presence of a game object at that pixel for the 'n' pixels of the generated maps. The other is the object loss 'L_o' which is used to approximate the deviation in proportions of the categories of the generated objects with that of the target objects of a level. It is obtained through finding the absolute sum error 'ϵ_{as}' of the generated feature maps from that of the target feature maps .

$$\epsilon_{as} = |\sum_{i=0}^{n} (X_{T\_True_i} - X_{T\_Gen_i})| \tag{4.5}$$

$$L_O = \mathbb{E}(\lambda \cdot ln|1 + \frac{\epsilon_{as}}{1 + \sum_{1=0}^{n} X_{T\_True_i}}) \tag{4.6}$$

This error is taken in proportion to the number of target objects to ensure that the categories with fewer objects do not get ignored. Natural log taken to modulate the extremely large values obtained from summing the map pixels with 'λ' used to amplify its significance. Finally, the mean of these losses is taken across the available categories as part of its summation with the GAN loss from Equation 2.8 and the mask loss to derive the total generator's loss.

$$L_{Gen} = \mathbb{E}_{x,z}[log(D(X_{I\_True}, X_{T\_Gen})] + L_O + L_M \tag{4.7}$$

4.4.2. Training Algorithm

The system is trained through iteratively executing the training operations over 1023 training samples 'X_{train}' with the models validated over the remaining 240 samples 'X_{Val}'. At the end of each epoch, reference samples are computed using the same seed of random noise with a mean of 0 and standard deviation of 1. These are used to provide a visual understanding as to the development of the model over the training cycle. As the architecture is composed of two separate models, the training algorithm has been distinctly tabulated with one detailing the processes performed by the WGAN network and another for the cGAN network.

This dataset is artificially enlarged for the WGAN networks to 8148 and 1840 for training and validation respectively through the consideration of the three 90-degree rotations and its mirror images to exploit for the differences in level orientation. Each of the WGAN networks has been trained for 100 epochs using a batch size of 16 with validation performed every 100 batches. The critic is trained for 3 steps for every step that the generator is trained instead of the suggested 5 but performs similarly when compared. A weight of 10 is multiplied to the gradient penalty for the critic loss. Both networks utilize Adam optimizers with a learning rate of 2e-4, beta decay of 0.5 and momentum set at 0.999.

Process	Inputs	Outputs	Periodicity	Evaluated Opertors
Train G	$Z_U[0,1]$	L_{G_Train}	3	X_{Gen}, Y_{Gen}
Train C	$X_{Train},$ $Z_U[0,1]$	L_{C_Train}	1	$X_{Gen}, Y_{Gen},$ Y_{Train}
Validation	$X_{Val},$ $Z_U[0,1]$	$L_{G\_Val},$ L_{C_Val}	300	$X_{Gen}, Y_{Gen},$ Y_{Val}
Reference Sample	Z_{Ref}	X_{G_Ref}	1512	-
Network Checkpoint	G, G_{Optim}	checkpoint	1512	-

Table 4.1: Training operation of WGAN models

The hybrid network on the other hand does not have its dataset enlarged since they are trained with a batch size of 1 and consecutive samples with altered orientations causes it to retain unnecessary bias when presented with unusual samples from the dataset. It is also trained over 100 epochs with validation performed every 100 batches, using the same hyperparameters with the exception being that the Adam optimizer has a learning rate of 6e-5 to reduce the impact of each batch and avoid reaching a local minimum.

Process	Inputs	Outputs	Periodicity	Evaluated Opertors
Train G	X_{I_Train}, $Z_U[0,1]$	L_{G_Train}	3	X_{T_Gen}, Y_{Gen}
Train C	X_{Train}, $Z_U[0,1]$	$L_{D_T rain}$	1	X_{T_Gen}, Y_{Gen}, Y_{Train}
Validation	X_{I_Val}, X_{T_Val}, $Z_U[0,1]$	L_{G_Val}, L_{D_Val}	100	X_{T_Gen}, Y_{Gen}, Y_{Val}
Metrics	X_{I_Val}, X_{T_Gen}	$metric_{eval}$	100	-
Reference Sample	X_{I_ref}, Z_{Ref}	X_{G_Ref}	1023	-
Network Checkpoint	G, G_{Optim}	checkpoint	1023	-

Table 4.2: Training operation of cGAN models

4.4.3.   Updated WAD Generator

Feature maps are used to reverse engineered into the mandatory lumps necessary for the DOOM engine with the help of certain refinements made to Giacomello's WAD Editor. Firstly, detached regions of the level have been addressed through the introduction of post processing before generation of category maps. It removes holes from the floor map and objects to ensure that map is fully connected before generating the corresponding map of the desired object categories. Another issue is the presence of untraversable paths that are caused by narrow corridors between the sections, making the observable section inaccessible. This happens when the scale size of pixel wide sectors is smaller than the player. It can be tackled by ensuring that the minimum size of each pixel corresponds to the dimensions of the character, enforcing a scaling factor 128 without exceeding the

bounds of the level space.

The Doom Engine also uses a Binary Space Partitioning Algorithm for pre-computing the Hidden Surface Determination or occlusion culling. In this work, the tool ZenNode [29] has been used in the last stage of the pipeline, to produce playable DOOM levels from the network output. ZenNode is a 3rd party software used to generate lumps that does not directly affect the level design. It has additional functionalities with a customizable Binary Space Partition to ignore certain LINEDEFs and specify unique SECTORs, though its main function is to provide incomplete PWADs with BLOCKMAP and REJECT resources automatically given that the remainder of the lumps have already been generated using the feature maps.

4.4.4.   Experimental Setup

The experiment performed is a comparative analysis between the proposed and prior architectures with traditional model added in to provide plausible justification for the inclusion of a more complex architecture in the hybrid network. While training the networks, similar models have been constructed near indistinguishable to minimize any variations that are not due to the inherent differences between the models. To this end, the networks use the same number of layers, hyperparameters, kernel size and stride wherever possible.

The experiment is set up initially to compare the cGAN networks through metrics performed during the training phase. Although it may seem tempting to simplify the functional generator by means of using just a UNET architecture which implementing the object and mask loss as discussed in the previous section, it is incapable of mimicking the subtle variations of object placements through performing the image-to-image translation purely with a fixed loss function and hence is rejected for this system.

The traditional WGAN-GP network is not taken into account for the training metrics as it does not use a two-step process making it difficult to calculate them without context. It also does not use the aforementioned category maps due to its generator's tendency towards producing predominantly zeros matrices for those features due to the sparse nature of the distribution. This architecture is found to at least be able to generate game objects up to a certain extent when trained with the things and has been included in the post training evaluation of the networks. Post training evaluation is done over 100 samples from the real and generated datasets.

Model	G_{Loss} Function	Feature Maps	G Convolutional Layers (filters)	D Convolutional Layers (filters)
WGAN	Wasserstien Distance with Gradient Penality	floormap, heightmap, wallmap, thingsmap	4 (1024, 512, 256, 128)	4 (128, 256, 512, 1024)
WGAN + Tradition cGAN	Wasserstien Distance with Gradient Penality	floormap, heightmap, wallmap	4 (1024, 512, 256, 128)	4 (128, 256, 512, 1024)
	Cross Entropy + $L1$ Norm	monstersmap, ammunitionsmap, powerupsmap, artifactsmap, weaponsmap	7 (128, 256, 512, 1024, 1024, 512, 256)	4 (128, 256, 512, 1024)
WGAN + Modified cGAN	Wasserstien Distance with Gradient Penality	floormap, heightmap, wallmap	4 (1024, 512, 256, 128)	4 (128, 256, 512, 1024)
	Cross Entropy + Object Loss + Mask Loss	monstersmap, ammunitionsmap, powerupsmap, artifactsmap, weaponsmap	7 (128, 256, 512, 1024, 1024, 512, 256)	4 (128, 256, 512, 1024)

Table 4.3: Trained architectures used for the comparative study

5 | Results

5.1. Evaluation Metrics

The focus of this portion of the thesis is to quantify the evaluation of the results that have been obtained from the experiments through the proposed metrics. The preliminary analysis is done to provide plausible justification for the use of the modified cGAN network through the training metrics that have been acquired alongside the validation to showcase their differences. The metrics consist of the discriminator's ability to classify the levels, the unique information needed to describe the level as well as the following statistics:

- Mean Object Count – It is the count of all objects within a level by the total area that the level occupies. It provides an approximate object density that is found in levels and serves as a constraint to check if the object maps are leaning towards over saturation or under saturation as the model must learn to balance increasing the availability of objects while avoiding overpopulating a level by making it too congested.

- Mean Encoding Error – Objects within the respective category maps are normalized between 0 and 1 with each object equidistant within the limits. The network generates images where pixels are encoded using continuous values which can be rounded towards the closest object type. As the networks use a ReLU activation function in the output layer due to the tendency of the cGANs with sigmoid activation towards predominately empty images, beyond the limits of assigned ids of the respective categories. This error is used to measure the inaccuracy in pixel values which would overflow into other categories if not addressed.

- Mean Out of bounds Error – When objects are generated outside the bounds of the level, they are ignored in the level generation process as they are inherently inaccessible to the player and thus not part of the actual level. This error is used to quantify how often this occurs and the degree to which the network is unable to comprehend the constraints within which game objects need to be placed.

It is difficult to compute the metrics during the training of the traditional WGAN since they are either require a definitive level structure which is not yet established as it is learning the complete distribution, making it impractical to compare their respective graphs. Instead a set of post training metrics are used to provide a more appropriate analysis. These include the performance of the generator in understanding the problem as well as the quality of object distribution, both spatially and categorically, which while not comprehensive, should provide conclusive evidence of its ability. These techniques assess the presence of a game object around the surrounding context, be it the local section or the encompassing level and are described as follows:

- Proportions Analysis – It is based on the proportions of the various categories based on the types of objects that it uses to populate the level. This is used to understand how well the model is able to grasp the relation between the requirement of placing objects from different categories and significance of their individual types. This in junction with the count of the individual object type from the available categories provide a clear picture on the biases and tendencies of the generator when selecting positive pixel's encoding.

- RipleyK Function – The spatial distribution of the generated objects can be measured using the Ripley's K function [26]. It determines whether points have a random, dispersed, or clustered distribution pattern. The function is calculated by taking the average occurrence of events within a predetermined radius of every point iteratively which provides an advantage over other methods since it is independent of the density of the point pattern and thus can describe the spatial point patterns at many different scales [41].

$$K(s) = \lambda^{-1} n^{-1} \sum_{i=1}^{n} \sum_{j \neq 1} I(d_{ij} < s) \tag{5.1}$$

  where 'd_{ij}' represents the distance between points 'i' and 'j', 's' is the threshold radius within which the point is considered and 'n' is the number of points that are sampled from the distribution with 'λ' being the reduction factor of the function.

Apart from these, there is also visual artifacts in the presentation of the things map that highlight the differences and can be used to distinguish the samples intuitively.

5.2.   Model Evaluation

5.2.1.   Training Metrics

By using the loss computed during the training sequence, we are able to compare the variation in the discriminators ability to identify the generated levels. As both the networks use different loss functions in their generators, it is difficult to directly compare their assessments and thus more emphasis will be given between graphs of discriminator in the cGAN networks from the hybrid architecture. Although validation data is not as useful in GANs to assess overfitting and/or implement early stopping, it is still done to hold back some real samples for testing the discriminating network to compare the how well it can classify images among the functional generators [33]. This can be seen in Figure 5.1 with the discriminator validation loss of the traditional cGAN rising above that of the traing around the 40th epoch while the network is only able to generate viable samples after the 80th epoch.
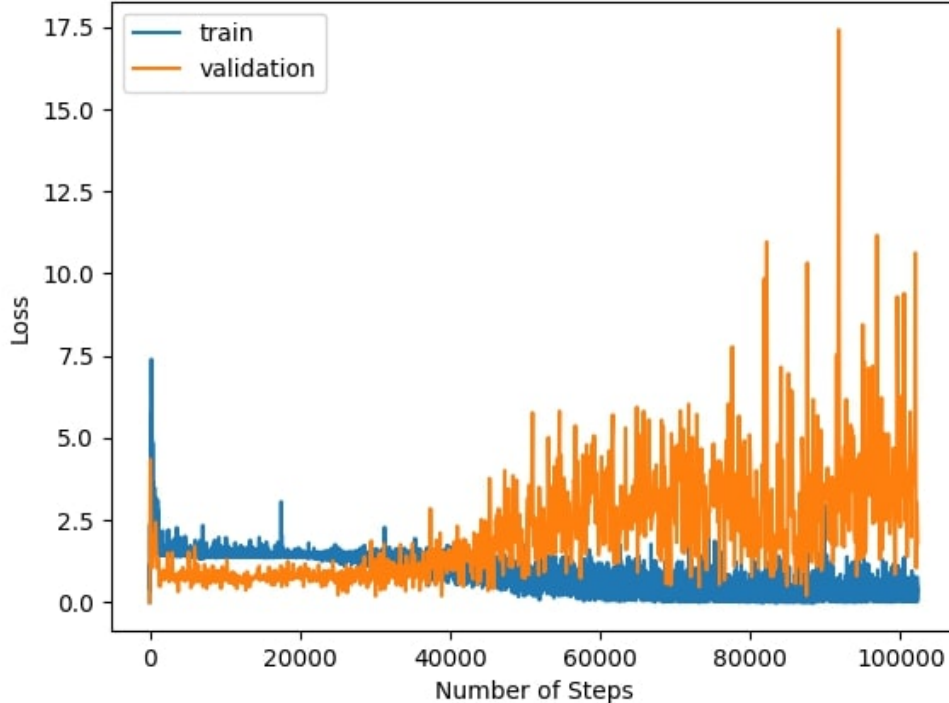
Figure 5.1: Discriminator Loss of the traditional cGAN model
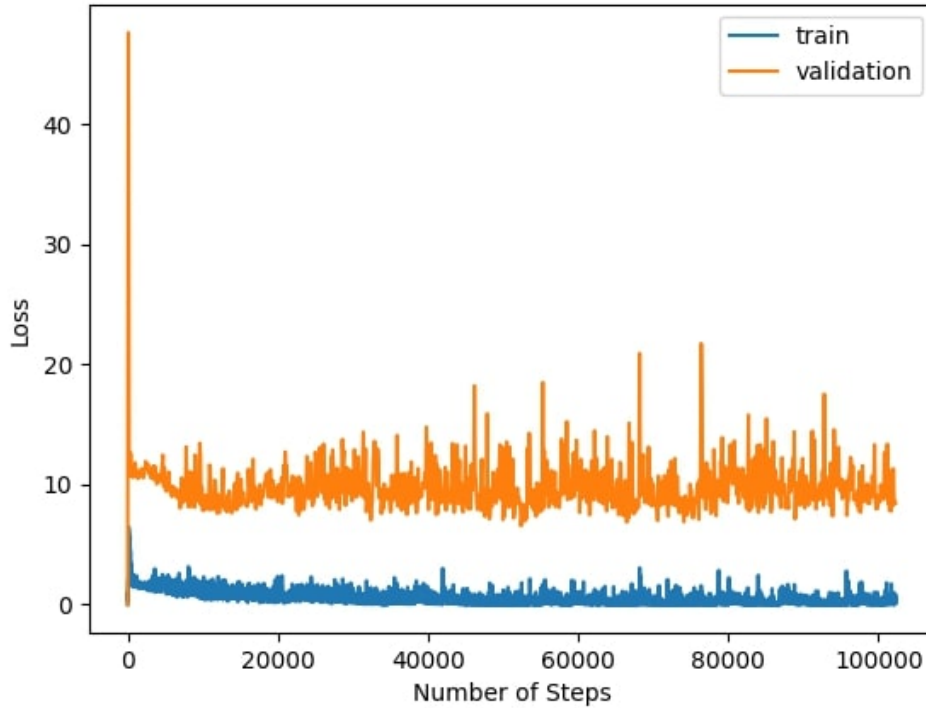
Figure 5.2: Discriminator Loss of the modified cGAN model

As seen in Figure 5.1 and Figure 5.2, the traditional cGAN is better at deceiving its discriminator with a smaller loss value but is plagued with inconsistencies due to the stricter constraints of the $L1$ norm present in the generator loss when handling outliers in the training dataset, leading to a more noisier graph when compared to the laxer restrictions imposed by the object and mask loss. This is also seen in the fact that the traditional cGAN performs very differently from each instance of the complete training cycle and seems to be extremely sensitive towards the shuffling process while the modified cGAN is able to repeatedly settle at a local minima that provides consistent results.
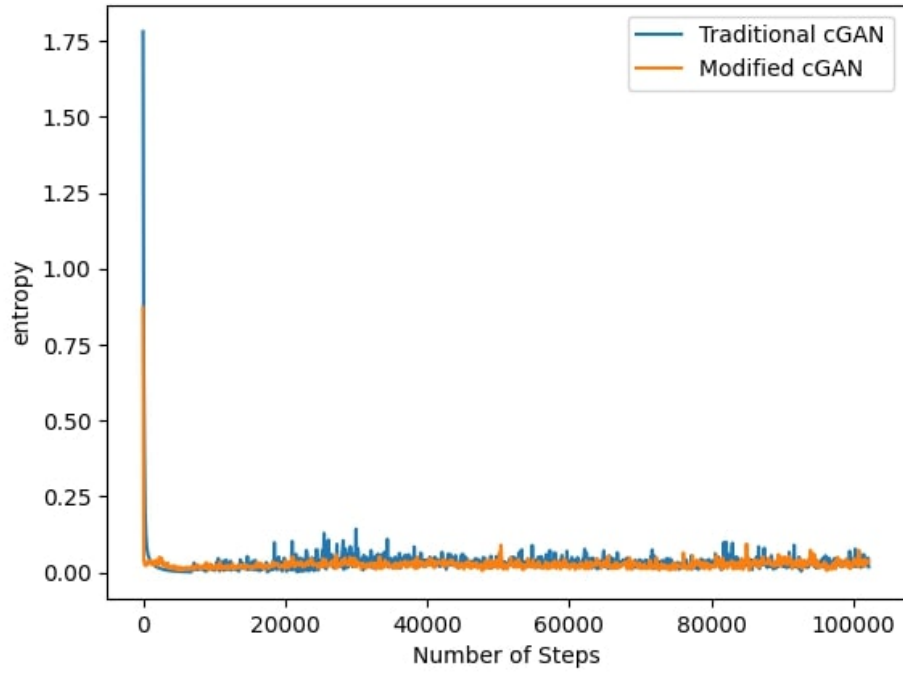
Figure 5.3: Mean entropy of the generated category maps
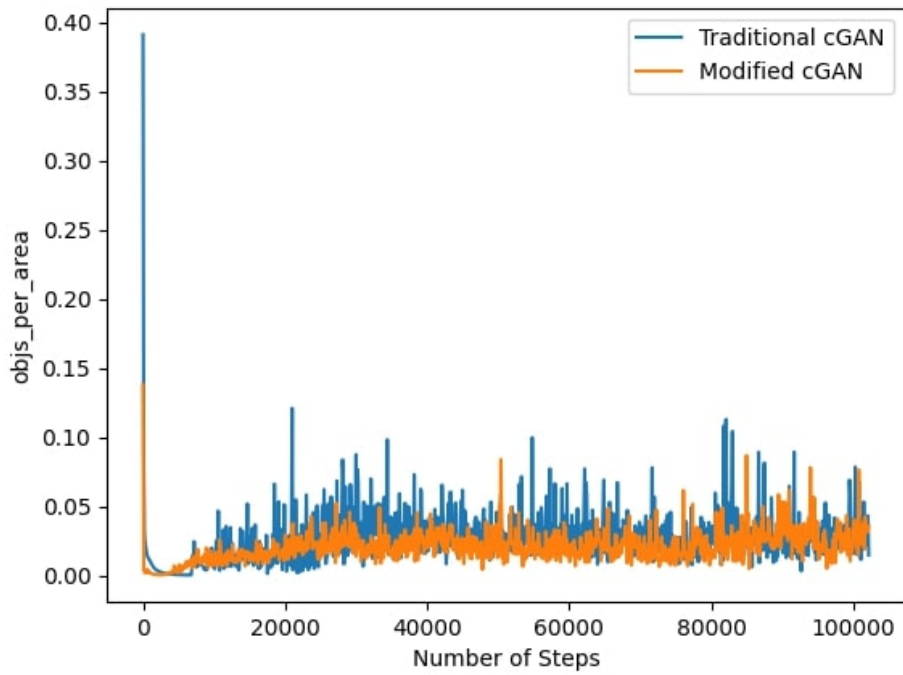
Figure 5.4: Mean object count per unit area of the generated category maps

Figure 5.3 and Figure 5.4 show the similarities between the cGAN networks with amount of randomness and the object counts being approximately the same during the training process which is misleading when not taken into context with the errors produced by the networks. The next set of metrics provide a better understanding of this inconsistency of the traditional cGAN with the encoding error showing lesser accuracy for assigning values within the limits of the object ids and the out of bounds error highlighting the positioning the objects outside the prescribed level space
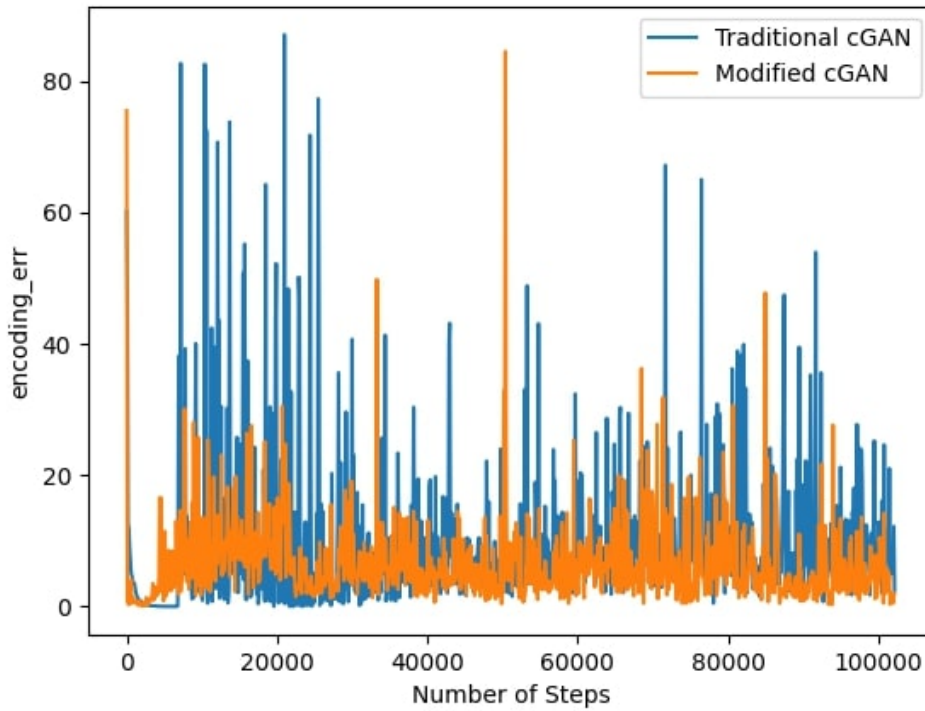
Figure 5.5: Mean encoding error of the generated category maps

Even though the traditional cGAN provides a object count in line with its modified counterpart, most of the objects that have been generated are not within the limit of the dictionary ids which has an negative effect to the otherwise normal object count after the correction made as seen in the generated maps. This is caused by outliers that occur within the feature maps of the repository because some custom levels having an unusual distribution such as higher count of more significant object types while only having fewer less significant object types.
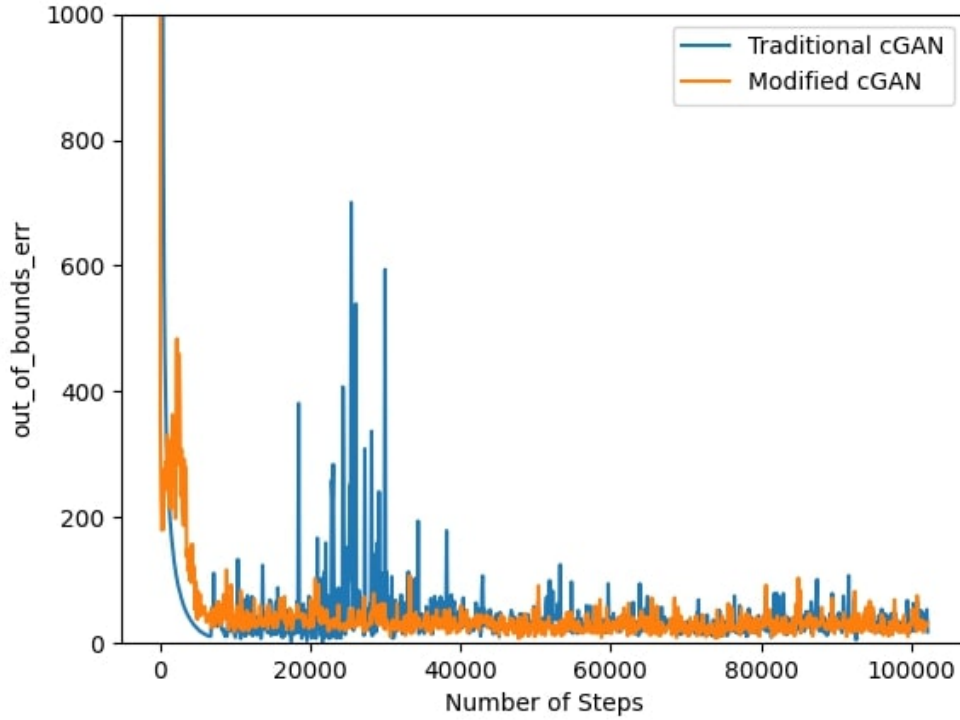
Figure 5.6: Mean out of bounds error of the generated category maps

The out of bounds error paints a similar picture with traditional cGAN suffering from the inability to generate objects within the predefined levels space consistently and this greatly vary among distinct repetitions of the training cycle as the dataset is shuffled differently at each instance. In an attempt to rectify, the network overcorrects which leads to the sensitivity that is noticed from before. There is also other issues that are encountered such as its ability to allot game object type less evenly among the categories by heavily favouring certain categories during the generation process. This is clearly visible in Figure 5.7 where the favoured category keeps varying throughout the multiple seperate repetitions of the training algorithm.

5.2.2. Proportions Analysis

By separating the problems, the hybrid architecture with a modified cGAN is shown to better learn the distribution of the various object categories while maintaining appropriate object density when compared to the traditional WGAN-GP as well as the traditional cGAN. Figure 5.7 shows the average proportions of categories among sampled from 100 game objects of the real and generated distributions of the thingsmap that have been taken into consideration. While the overall proportions are a major concern in determining the quality of gameplay, there is also a need to moderate the intensity created by the individual object based on the type within the category. As such boss level monsters or the BFG 3000 require a much more appropriate environment to appreciate its presence and must be reflected in the number present in each level. In such cases, the modified cGAN adheres to these principles and sparingly generates such objects which can be observed in Appendix A that provides average count of each object for every category within the levels.
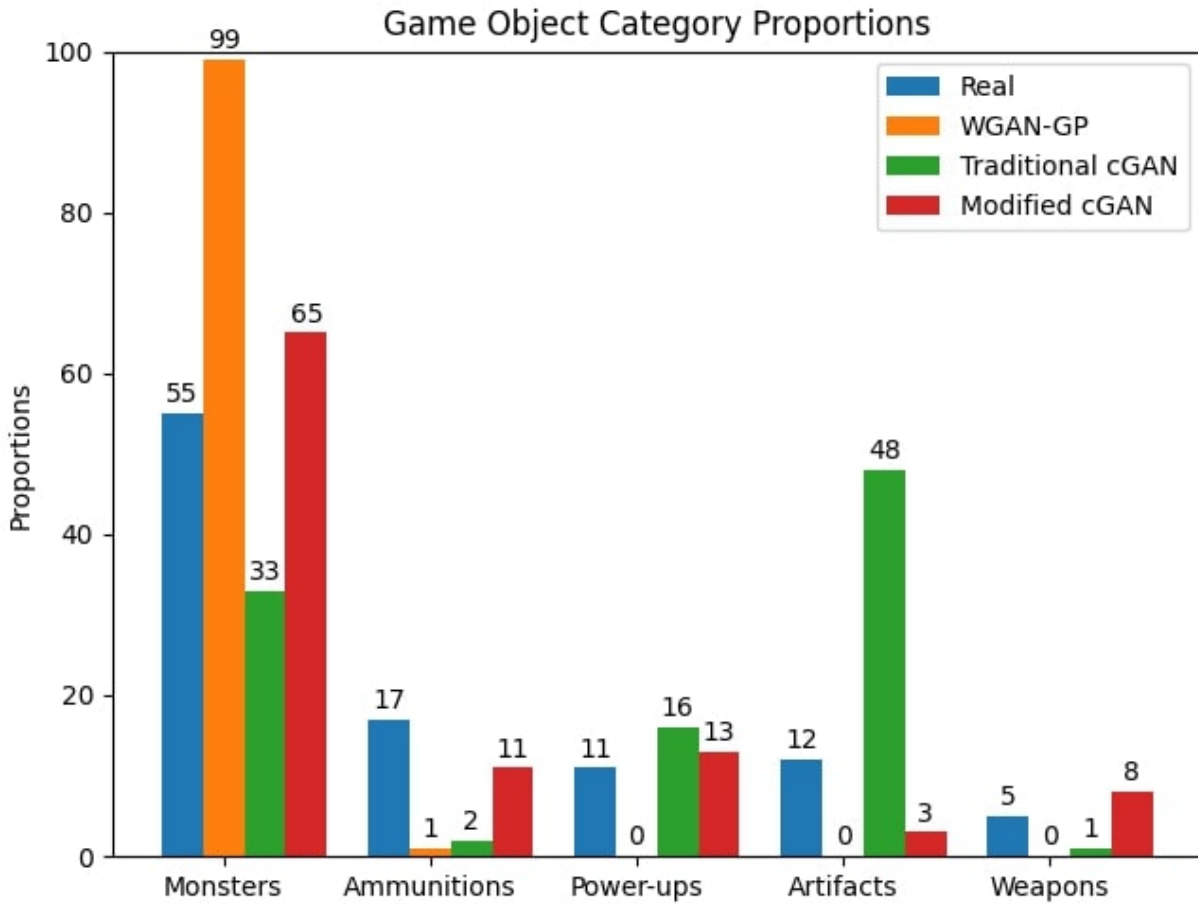
Figure 5.7: Average proportions of each category for sampled levels

5.2.3.   Spatial Homogeneity

The results are interpreted with larger values being the outcome of distributions that have greater deviation to completely spatial random distributions which are spread homogenously across the given space. Table 5.1 records the average spread of the objects with the results closest to the real distribution being that of the Modified cGAN architecture. It is measured at various radii with the histograms of all of the networks at each radius provided in Appendix B. This is done as points have a greater tendency to cluster or spread when focusing on larger or smaller portions than compared to the actual size of the normalized maps [31].

Radius	Real Distribution	WGAN-GP	Traditional cGAN	Modified cGAN
0.5	0.30652046	0.9182727	0.2539922	0.2790264
0.6	0.3121132	0.9833668	0.2227212	0.2916092
0.7	0.3097486	1.01664615	0.2105812	0.2953739
0.8	0.29492097	1.0403639	0.1642932	0.2772668
0.9	0.2699137	1.0340037	0.0897885	0.2393177
1.0	0.2367517	1.0010820	0.02104355	0.2059285

Table 5.1: Average Ripley K value taken at multiple radii

The traditional WGAN network has a greater average ripley-K result at each of the radii due to overly clumping its game objects near the walls its level structure. This drastically reduces through the use of either cGAN network as it provides a more homogeneous distribution which is in line with that shown by the results from the real feature maps and is why they both lead to a similar result.

5.3. Sample Generation

5.3.1. Traditional WGAN-GP Model
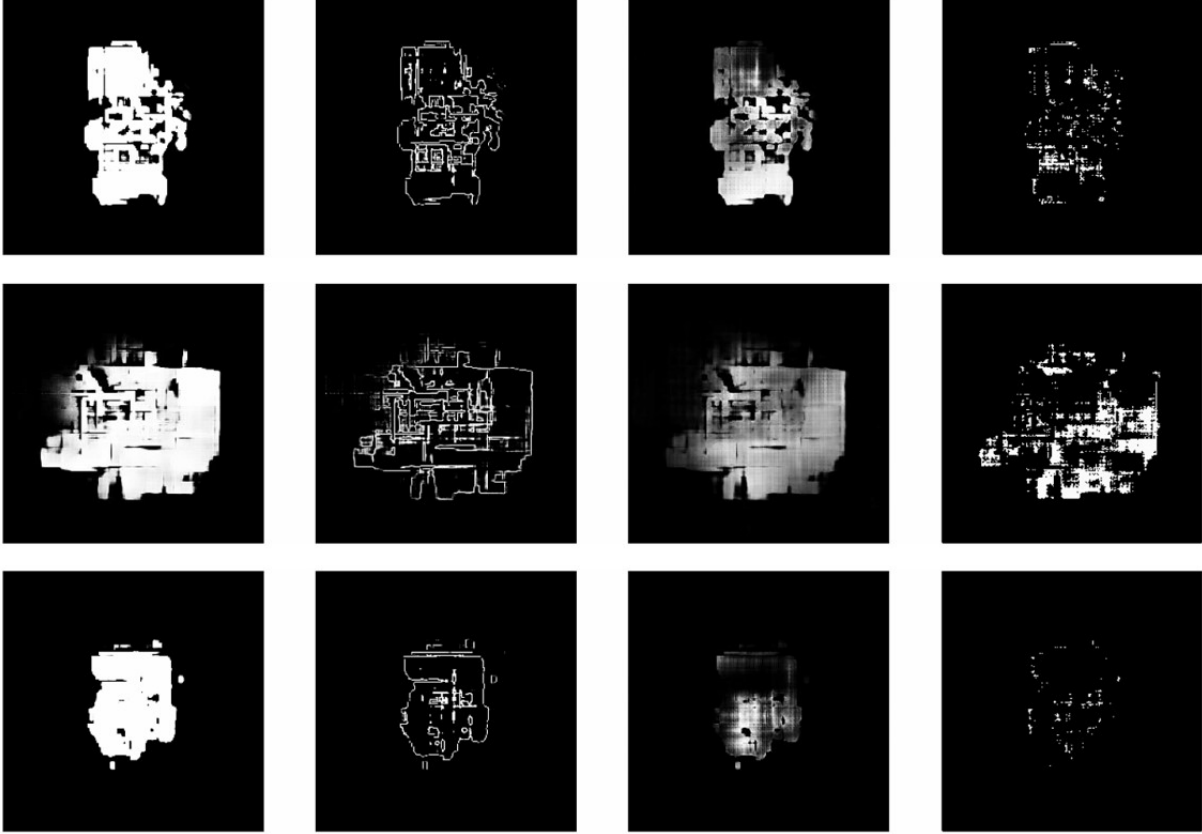
Figure 5.8: Floor map, Height map, Wall map and Things map (columns) generated using the traditional WGAN-GP architecture

As seen here, the traditional WGAN-GP network trained is capable of interpreting relations between the wall and floor layouts as well as provide the height of the various sections but is unable to capture the distribution of the various game objects across the level due to the increased complexity of the problem. As such there occurs a disparity in the distribution of game objects among the categories by mostly generating objects for the first category of the sequenced dictionary id with emphasis towards lower values. This is better in comparison to providing the expanded feature map as it usually generated zero matrices for those feature maps.
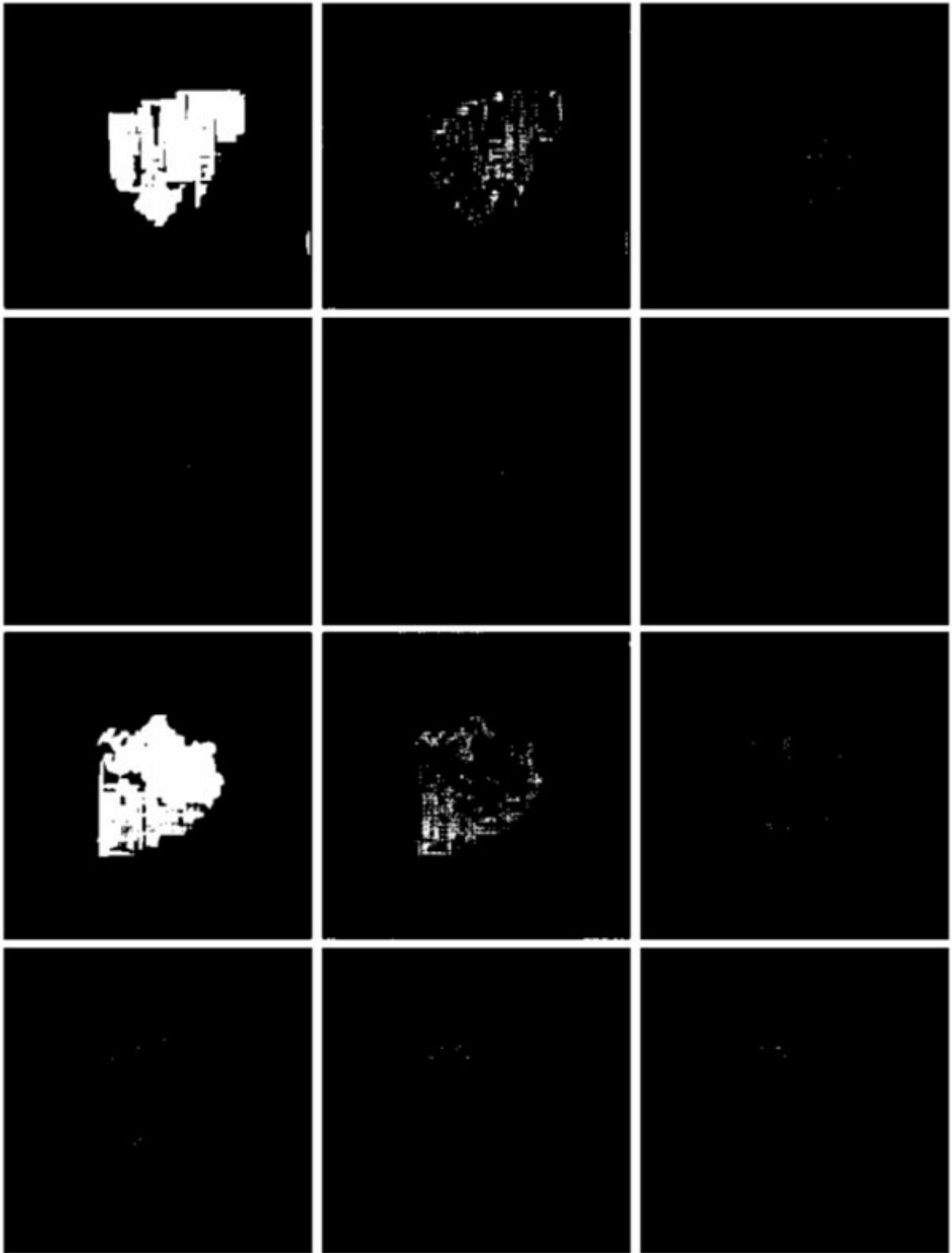
Figure 5.9: Floor, Monsters, Ammunitions, Powerups, Artifacts and Weapons Map (Column pairs) generated using the traditional WGAN-GP network (1 of 2)
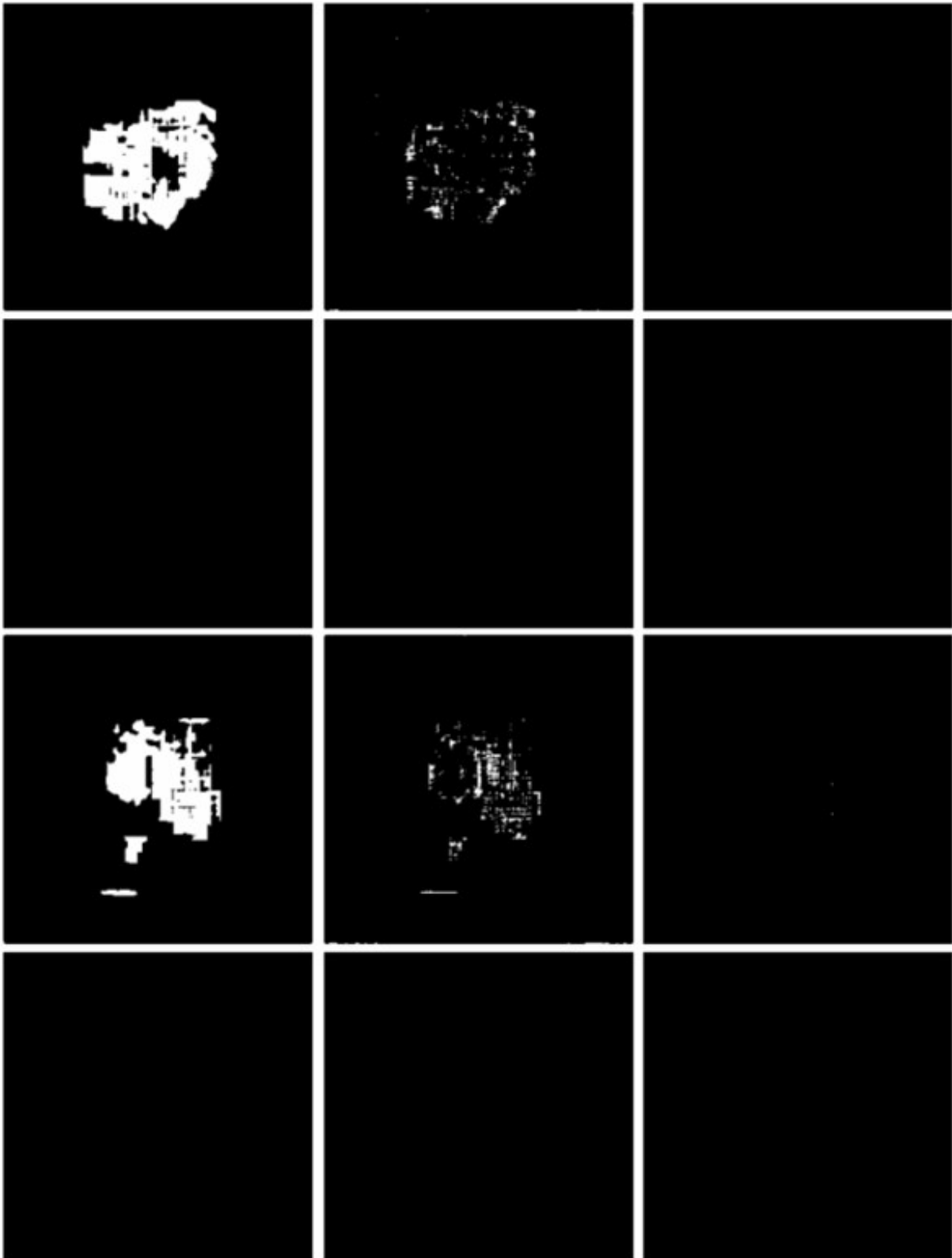
Figure 5.10: Floor, Monsters, Ammunitions, Powerups, Artifacts and Weapons Map (Column pairs) generated using the traditional WGAN-GP network (2 of 2)

5.3.2.   Hybrid Model with Traditional cGAN
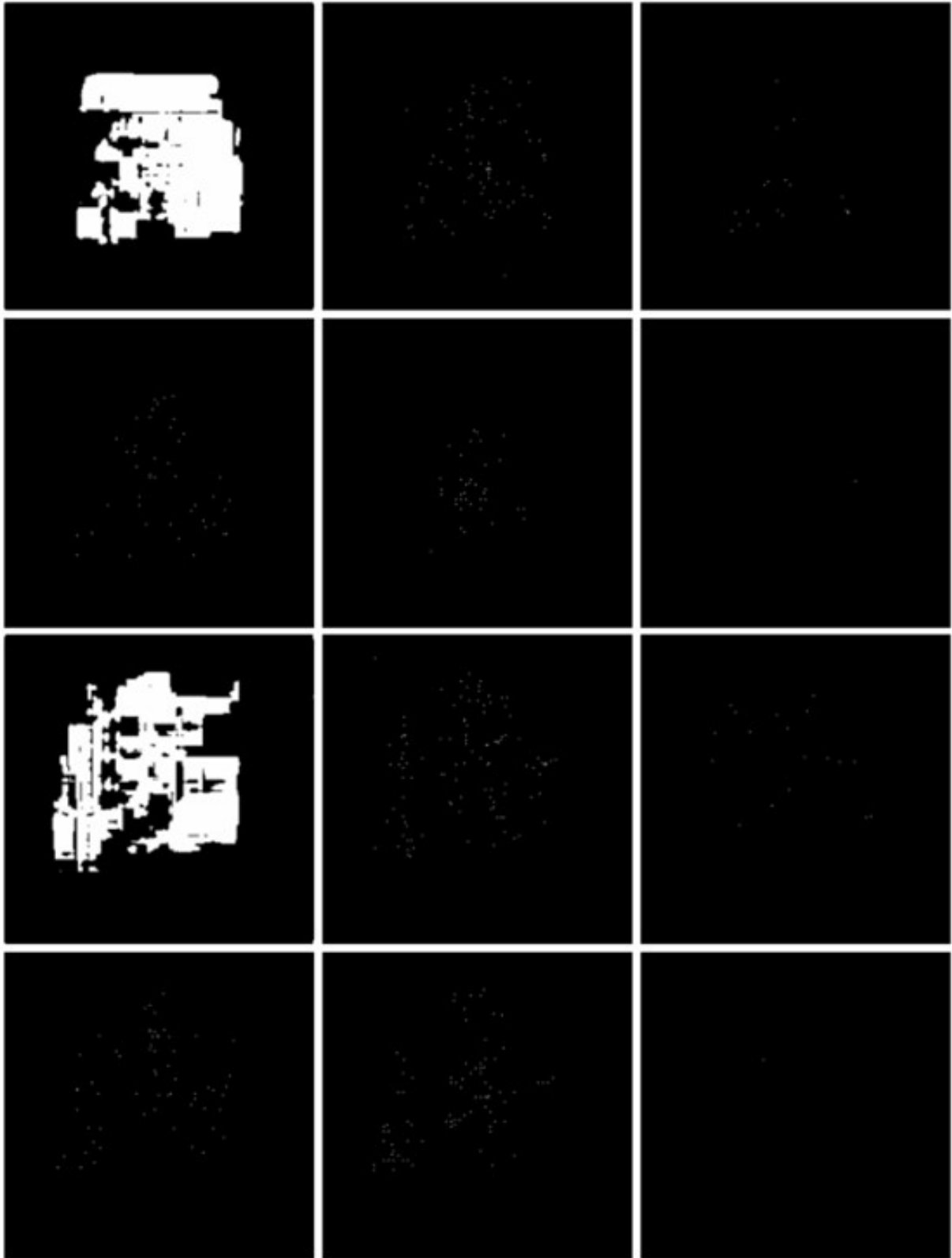
Figure 5.11: Floor, Monsters, Ammunitions, Powerups, Artifacts and Weapons Map (Column pairs) generated using the hybrid architecture with traditional cGAN network (1 of 2)
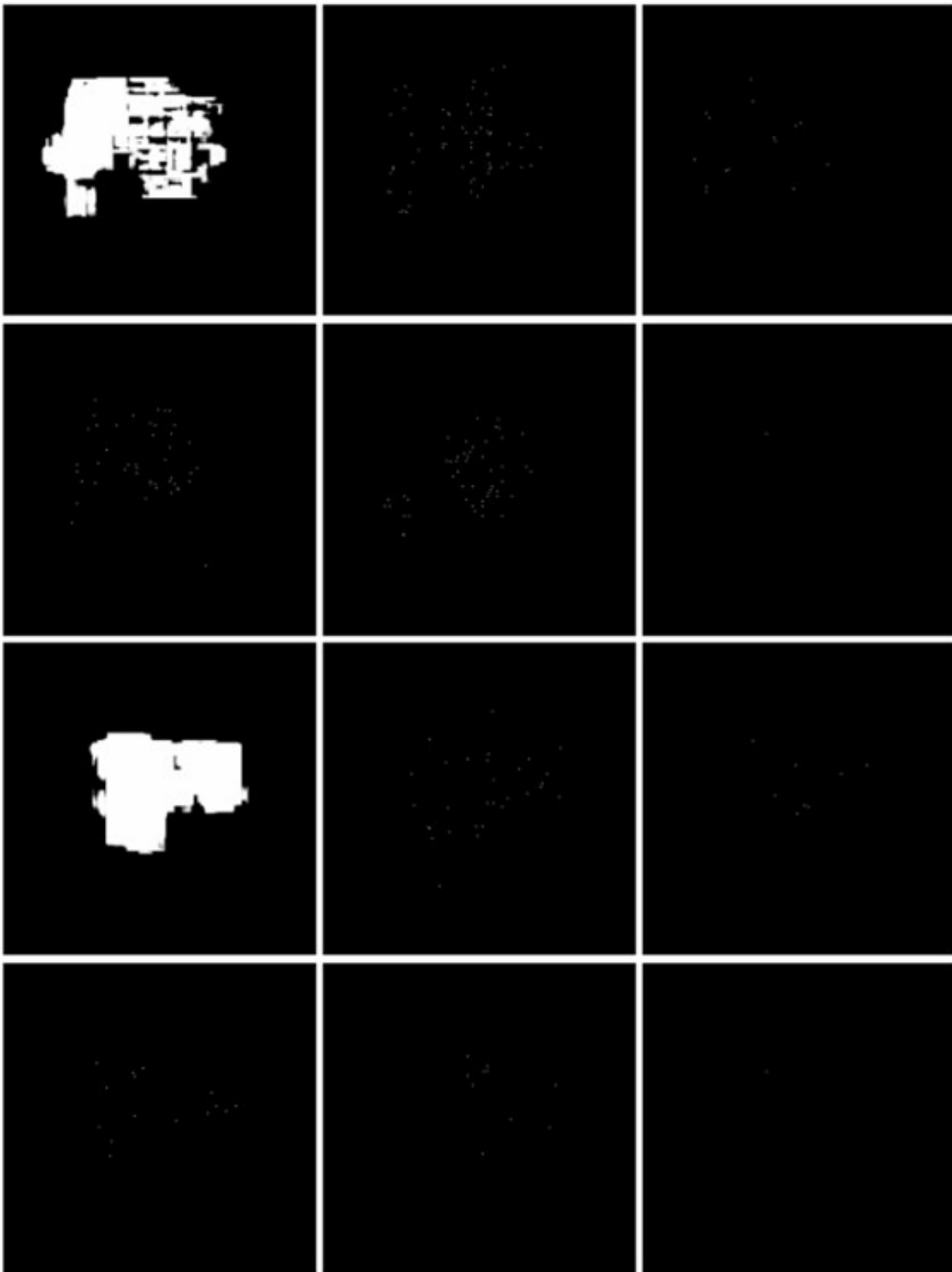
Figure 5.12: Floor, Monsters, Ammunitions, Powerups, Artifacts and Weapons Map (Column pairs) generated using the hybrid architecture with traditional cGAN network (2 of 2)

5.3.3.   Hybrid Model with Modified cGAN
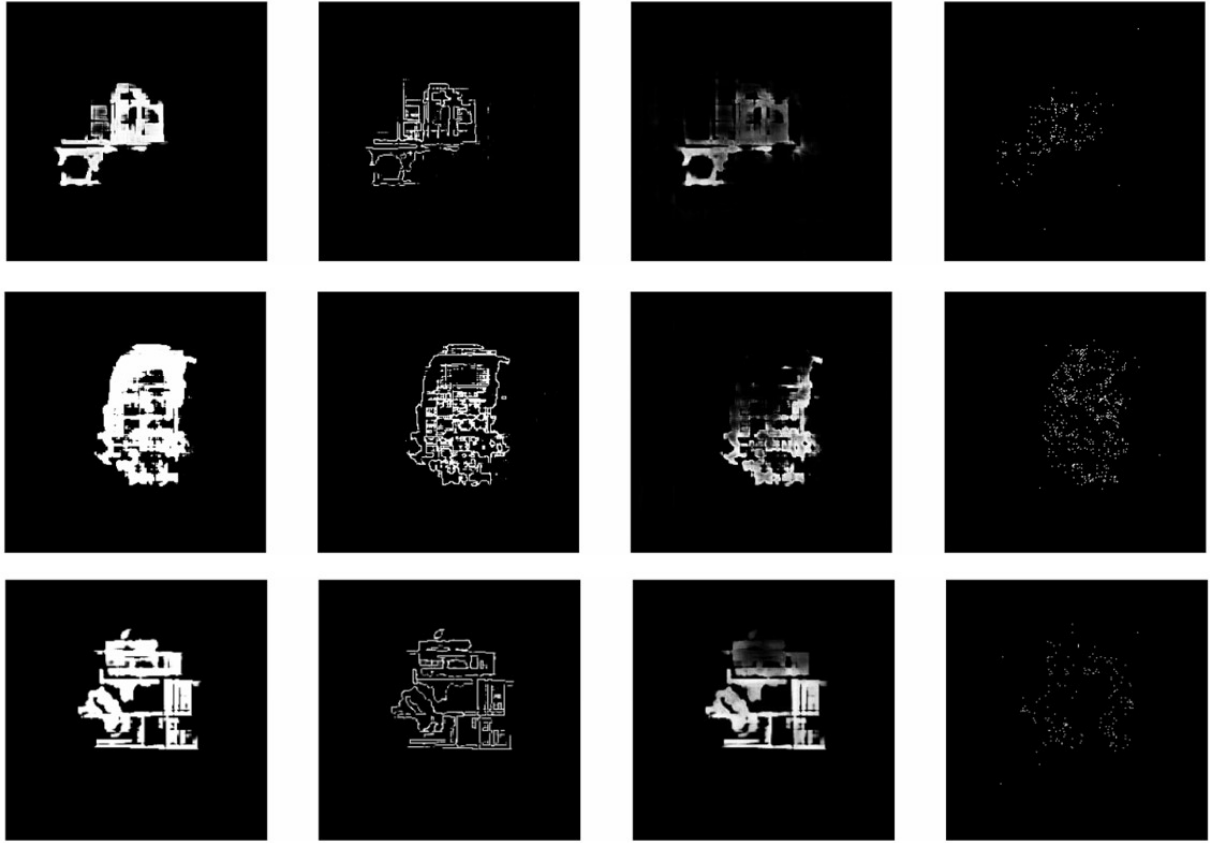
Figure 5.13: Floor map, Height map, Wall map and Things map (rows) generated using the hybrid architecture with modified cGAN network

The hybrid network works around this by separating it into 2 distinct subproblems, allocating the WGAN to focus primarily on the level structure while the cGAN network maps the object positions from the generated level structure. This also allows the WGAN to focus more resources towards learning the topological distribution which helps in the development of better level layouts to a certain extent. This does not ensure that its structure is always better given a random seed as the samples that have been use have been handpicked and showcases the best of both networks. As both hybrid models use the same WGAN generator, the topological maps are same with the only difference lying in its expanded object maps.
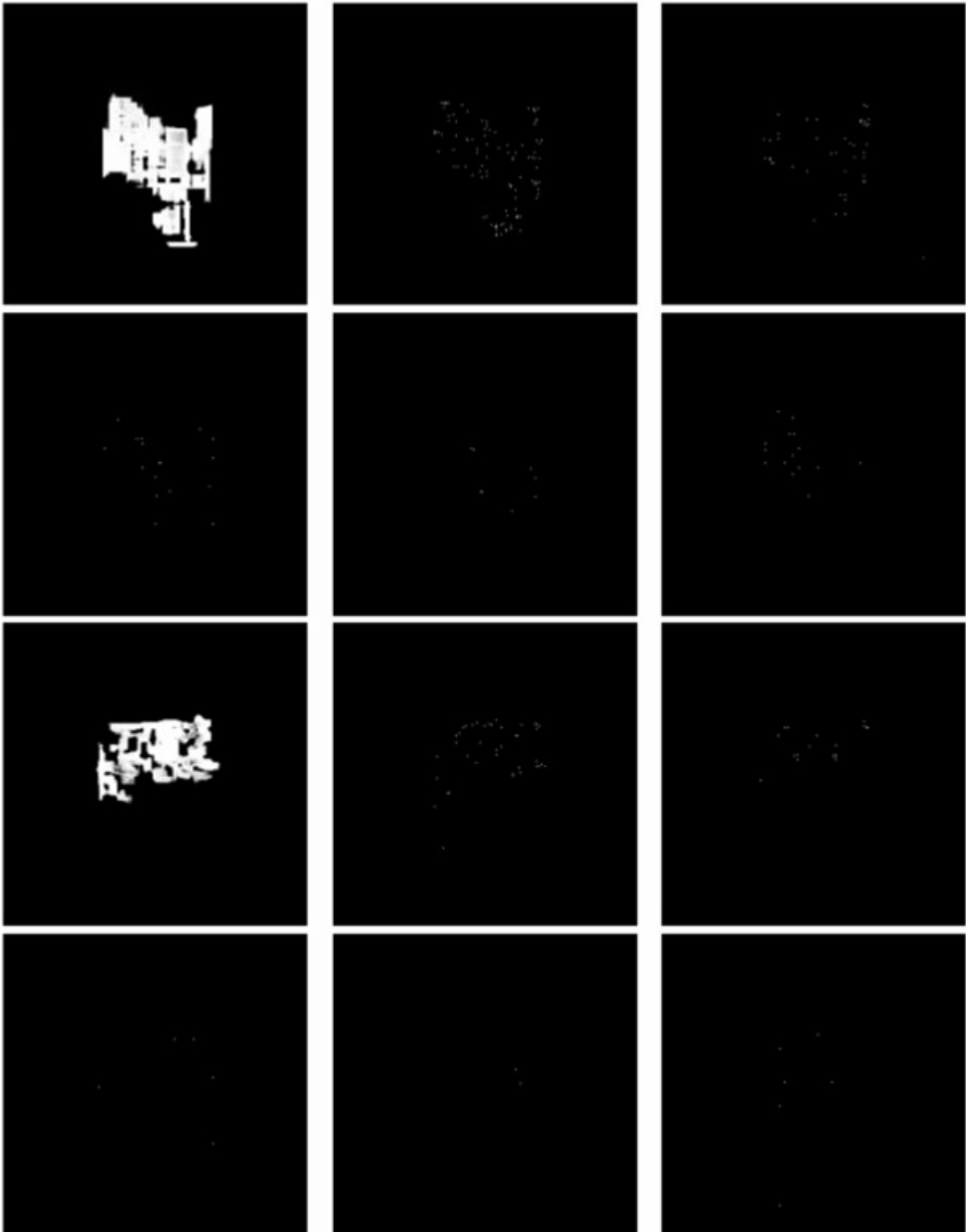
Figure 5.14: Floor, Monsters, Ammunitions, Powerups, Artifacts and Weapons Map (Column pairs) generated using the hybrid architecture with modified cGAN network (1 of 2)
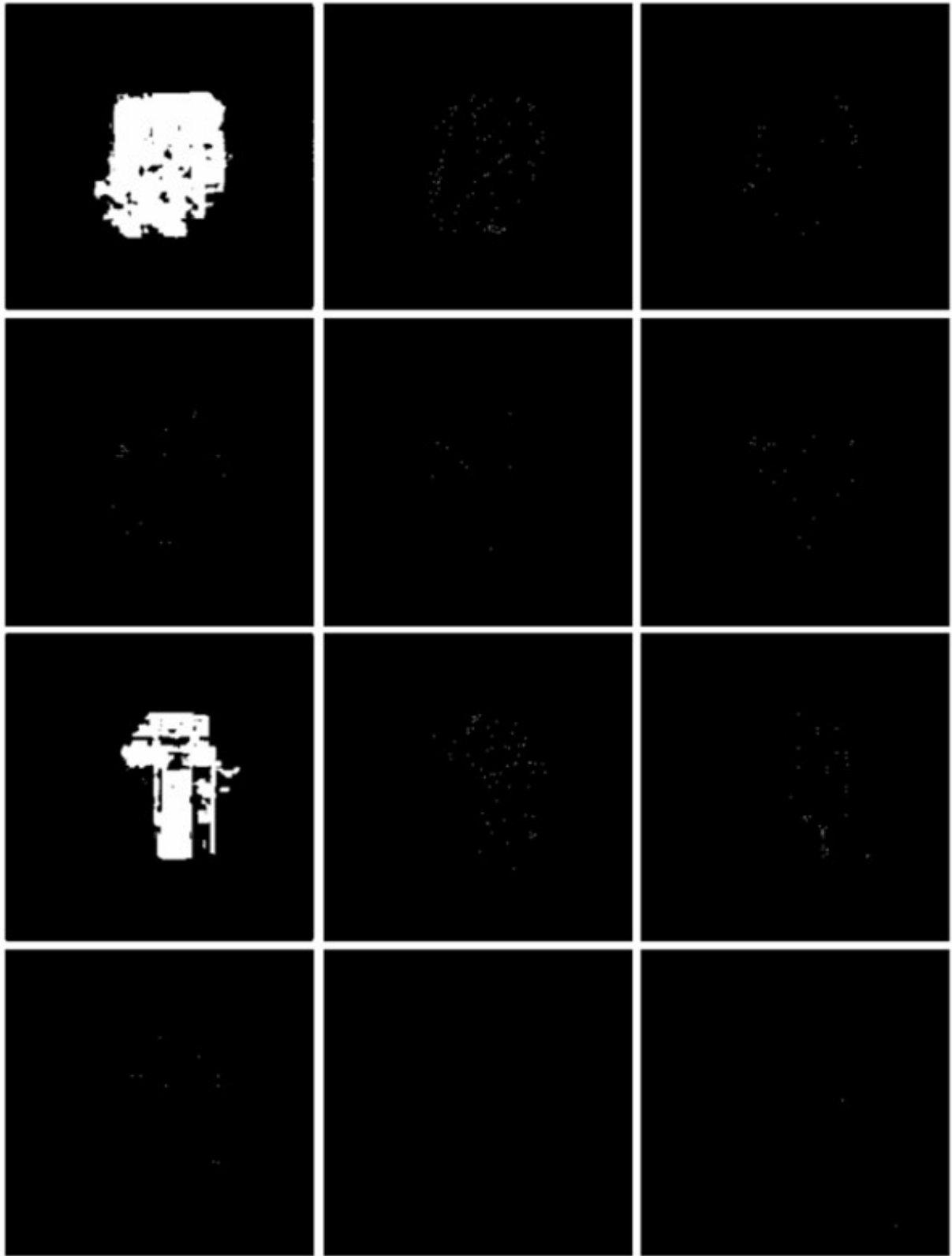
Figure 5.15: Floor, Monsters, Ammunitions, Powerups, Artifacts and Weapons Map (Column pairs) generated using the hybrid architecture with modified cGAN network (2 of 2)

5.3.4.   Condensed Category Map Comparison
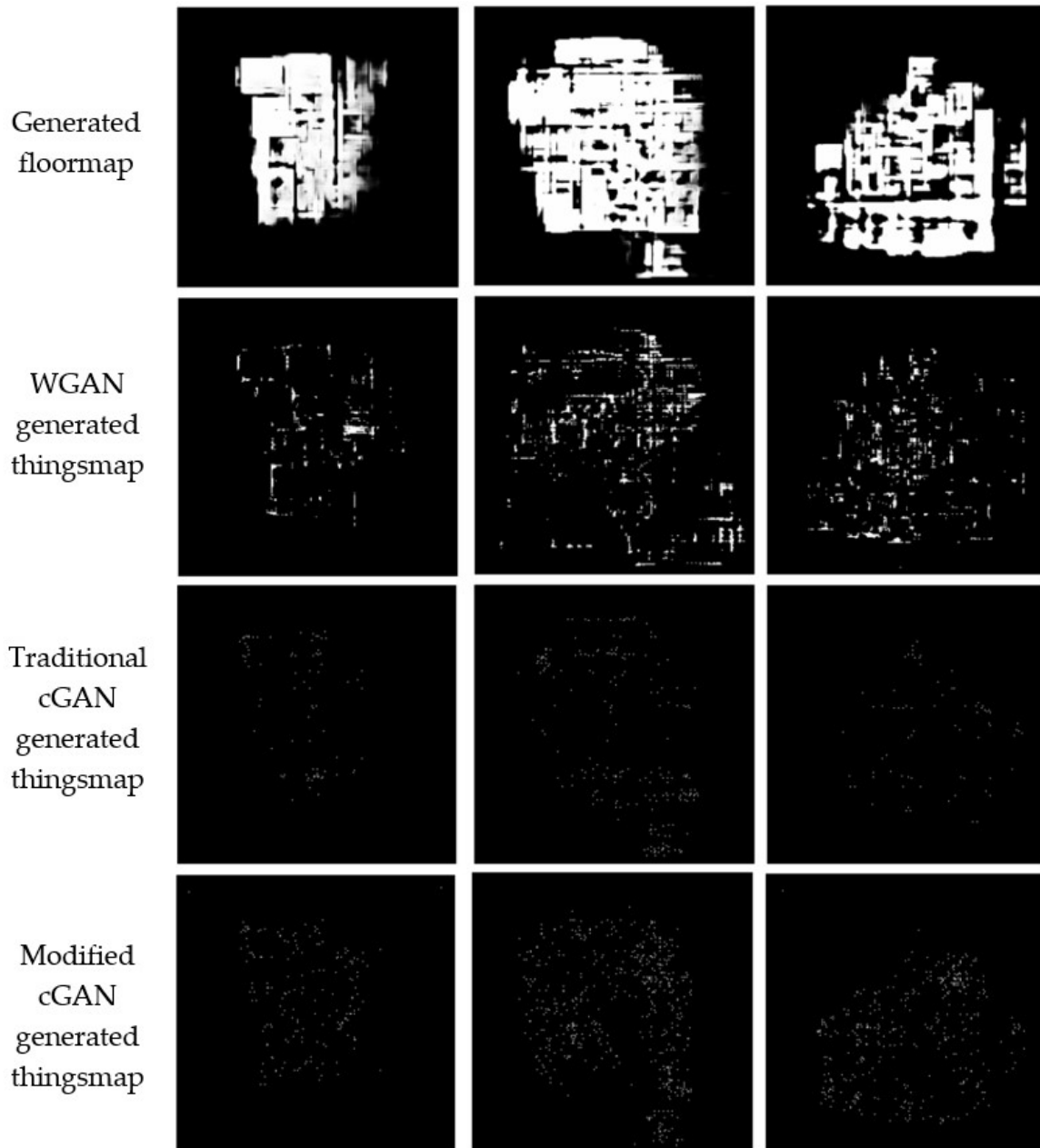
Figure 5.16: Generated things maps of the various models using levels generated by the WGAN-GP

6 | Conclusion

The above system should serve as an early prototype for a more holistic format procedural generation of 3D levels using generative adversarial networks. The hybrid system has shown its prowess to suitably provide objects within a given level space and has solved any issues that could hinder gameplay from the previous design. It has proven in its ability to provide the minimum subset of features needed to capture all the fundamental aspects of a level that can be exercised in isometric game engines by taking advantage of the simplicity of level structure in earlier games. This can be replicated in most games with a 2D map system to improve their replayability through the generation of multiple level layouts as well as multiple game object maps for each layout occasionally.

The models in this experiment are restrained in using the same dataset for the sake of remaining consistent across all of the trained architectures. The system is open to improvement by modifying the dataset so that each model within the hybrid architecture can be fully utilized to its utmost potential. This can be done simply by altering the dataset that is used to train each of the models by tailoring it towards their strengths by means of reducing the image size and dropping the padding entirely for the WGAN-GP subsystem while making use of this preprocessing for the cGAN. This model can also incorporate other categories present within DOOM object types such as the obstacles and decorations.

While there are certain limitations and room for improvement, it stands as a better alternative to games that rely on 'grinding' the same maps to slow the pace at which the player progresses through its content and finishes a game earlier which might indirectly affect the brand image. There is also the added benefit of reducing the excessive dependence on content developers to design every level with intricate details to maximize content by relying on such systems to provide generic levels as buffers between impactful locations to allow for all around better pacing within games.

6.1.   Limitations

There are a few constraints regarding its applicability to other games as it requires game data to be stored in a format where level structures can be easily decoded and parsed into image maps manually or through level builders with detailed specifications or guides. This system is dependent on the game having a large collection of level instances created either by the studio or through effective tools for the community to build, access and share. The system is also unable to represent multiple floors or stacked sections which are required to construct native 3D maps. The system does not allow for different noisy images to consistently generate significantly different category maps as there are usually very slight differences in their placements. There is also an issue in implementing doors and keys which need to be addressed as well as the use teleporters to connect detached segments within the level layout by including the respective triggers and landings before they can be used to develop the aspect of puzzles with the game play.

6.2.   Future Works

This system can be expanded by implementing additional models to separately learn the texture distribution of the level with the texture maps implemented through encoding pixels with texture id from a graphic dictionary and used to generate by means of a conditional network as used here. Conversely, by modifying the architecture to represent the textures map at lower resolutions, actual pixel colors can be encoded in the images to generate new graphics that are then extracted from the maps and encoded to their respective formats. Although this requires image translation with super resolution models [40] that can generate the aesthetical features together as the process would be dramatically upscaled for representing the complete texture map at an acceptable resolution.

By adding relations between pair of objects such as teleporters and landings or locked doors and keys that can be introduced through a separate feature map representation, it can be used to improve the versatility of the generator to be used in other genres as long as steps are taken to ensure that the levels generated meets the standard requirements such as solvability through additions made in the shortest path algorithms when considering these objects. The system can also be modified with different sets of objects and used to train agents within simulated environments by learning a possible set actions or behaviors given certain objects present in them.

Bibliography

[1] M. Arjovsky, S. Chintala, and L. Bottou. Wasserstein gan. *ICML'17: Proceedings of the 34th International Conference on Machine Learning*, 70:214–223, 08 2017.

[2] C. Beckham and C. Pal. A step towards procedural terrain generation with gans. *34th International Conference on Machine Learning(ICML*, 08 2017.

[3] D. Braben and I. Bell. Elite, 1984. game.

[4] Y. Chen, I. Keivanloo, and C. Roy. Near-miss software clones in open source games: An empirical study. *Canadian Conference on Electrical and Computer Engineering*, pages 1–7, 05 2014. doi: 10.1109/CCECE.2014.6901018.

[5] S. Earle. Using fractal neural networks to play simcity 1 and conway's game of life at variable scales, 01 2020. URL `https://arxiv.org/abs/2002.03896`.

[6] M. Fell. The unofficial doom specs, 1994. URL `https://www.gamers.org/dhs/helpdocs/dmsp1666.htmlc`.

[7] T. Frattesi, D. Griesbach, J. Leith, and T. Shaffer. Replayability of video games. Master's thesis, Worcester Polytechnic Institute, Worcestershire, England, 05 2011.

[8] H. Games. No man's sky, 2016. game.

[9] E. Giacomello, P. L. Lanzi, and D. Loiacono. Doom level generation using generative adversarial networks. pages 316–323, 2018. doi: 10.1109/GEM.2018.8516539.

[10] I. Goodfellow, J. Pouget-Abadie, M. Mirza, B. Xu, D. Warde-Farley, S. Ozair, A. Courville, and Y. Bengio. Generative adversarial networks. *Advances in Neural Information Processing Systems*, 3, 06 2014. doi: 10.1145/3422622.

[11] I. Gulrajani, F. Ahmed, M. Arjovsky, V. Dumoulin, and A. Courville. Improved training of wasserstein gans. *NIPS'17: Proceedings of the 31st International Conference on Neural Information Processing Systems*, page 5769–5779, 12 2017.

[12] M. Hendrikx, S. Meijer, J. Velden, and A. Iosup. Procedural content generation for

games: A survey. *ACM Transactions on Multimedia Computing, Communications, and Applications (TOMCCAP)*, 9, 02 2013. doi: 10.1145/2422956.2422957.

[13] S. Hochreiter and J. Schmidhuber. Long short-term memory. *Neural computation*, 9:1735–80, 12 1997. doi: 10.1162/neco.1997.9.8.1735.

[14] P. Isola, J.-Y. Zhu, T. Zhou, and A. Efros. Image-to-image translation with conditional adversarial networks. pages 5967–5976, 07 2017. doi: 10.1109/CVPR.2017.632. URL https://doi.ieeecomputersociety.org/10.1109/CVPR.2017.632.

[15] S. Karakovskiy and J. Togelius. The mario ai benchmark and competitions. *Computational Intelligence and AI in Games, IEEE Transactions on*, 4:55–67, 03 2012. doi: 10.1109/TCIAIG.2012.2188528.

[16] D. Karavolos, A. Liapis, and G. Yannakakis. A multifaceted surrogate model for search-based procedural content generation. *IEEE Transactions on Games*, 13(1): 11–22, 2021. doi: 10.1109/TG.2019.2931044.

[17] T. Karras, S. Laine, and T. Aila. A style-based generator architecture for generative adversarial networks. *CoRR*, abs/1812.04948:4396–4405, 06 2019. doi: 10.1109/ CVPR.2019.00453. URL http://arxiv.org/abs/1812.04948.

[18] A. Khalifa, P. Bontrager, S. Earle, and J. Togelius. Pcgrl: Procedural content generation via reinforcement learning. *CoRR*, abs/2001.09212, 01 2020. URL https://arxiv.org/abs/2001.09212.

[19] G. Lample and D. Chaplot. Playing fps games with deep reinforcement learning. *CoRR*, abs/1609.05521, 09 2016. URL http://arxiv.org/abs/1609.05521.

[20] Z. Li, S. Zhu, B. Shao, X. Zeng, T. Wang, and T.-Y. Liu. Dsn-ddi: an accurate and generalized framework for drug–drug interaction prediction by dual-view representation learning. *Briefings in Bioinformatics*, 24, 01 2023. doi: 10.1093/bib/bbac597.

[21] J. Liu, S. Snodgrass, A. Khalifa, S. Risi, G. Yannakakis, and J. Togelius. Deep learning for procedural content generation. *Neural Computing and Applications*, 33 (1):19–37, 10 2020. doi: 10.1007/s00521-020-05383-8. URL https://doi.org/10. 1007/2Fs00521-020-05383-8.

[22] W. McCulloch and W. Pitts. A logical calculus of the ideas immanent in nervous activity. *Bulletin of Mothemnticnl Biology*, 52(1/2):99–115, 1990. URL http:// arxiv.org/abs/1706.03762.

[23] MicroProse. Civilization ii, 1996. game.

[24] K. Park, B. W. Mott, W. Min, K. E. Boyer, E. N. Wiebe, and J. C. Lester. Generating educational game levels with multistep deep convolutional generative adversarial networks. pages 1–8, 2019. doi: 10.1109/CIG.2019.8848085.

[25] A. Radford, L. Metz, and S. Chintala. Unsupervised representation learning with deep convolutional generative adversarial networks. 11 2016. URL `http://arxiv.org/abs/1511.06434`.

[26] B. D. Ripley. The second-order analysis of stationary point processes. *Journal of Applied Probabilityg*, 13:255–266, 06 1976. doi: 10.2307/3212829.

[27] R. Rombach, A. Blattmann, D. Lorenz, P. Esser, and B. Ommer. High-resolution image synthesis with latent diffusion models. pages 10674–10685, 06 2022. doi: 10.1109/CVPR52688.2022.01042. URL `https://doi.ieeecomputersociety.org/10.1109/CVPR52688.2022.01042`.

[28] O. Ronneberger, P. Fischer, and T. Brox. U-net: Convolutional networks for biomedical image segmentation. *LNCS*, 9351:234–241, 10 2015. doi: 10.1007/978-3-319-24574-4_28.

[29] M. Rousseau. Zennode, 2004. URL `https://www.mrousseau.org/programs/ZenNode/`. node,blockmap,reject builder.

[30] A. Sauer, K. Chitta, J. Muller, and A. Geiger. Projected gans converge faster. *CoRR*, abs/2111.01007, 2021. URL `https://arxiv.org/abs/2111.01007`.

[31] J. Sporring, R. Waagepetersen, and S. Sommer. Generalizations of ripley's k-function with application to space curves. *26th International Conference on Information Processing in Medical Imaging (IPMI)*, 11492:731–742, 12 2018.

[32] A. Summerville, M. Guzdial, M. Mateas, and M. Riedl. Learning player tailored content from observation: Platformer level generation from video traces using lstms. 12:107–113, 06 2021. doi: 10.1609/aiide.v12i2.12895. URL `https://ojs.aaai.org/index.php/AIIDE/article/view/12895`.

[33] D. Talwar, S. Guruswamy, N. Ravipati, and M. Eirinaki. Evaluating validity of synthetic data in perception tasks for autonomous vehicles. pages 73–80, 08 2020. doi: 10.1109/AITEST49225.2020.00018.

[34] J. Togelius, G. N. Yannakakis, K. O. Stanley, and C. Browne. Search-based procedural content generation: A taxonomy and survey. *IEEE Transactions on Computational Intelligence and AI in Games*, 3(3):172–186, 2011. doi: 10.1109/TCIAIG.2011.2148116.

[35] M. Toy and G. Wichman. Rogue, 1980. game.

[36] Y. Tsujino and R. Yamanishi. Dance dance gradation: A generation of fine-tuned dance charts. *17th IFIP TC 14 International Conference, WCC 2018*, pages 175–187, 08 2018. doi: 10.1007/978-3-319-99426-0_15.

[37] T. Tutenel, R. M. Smelik, R. Lopes, K. J. de Kraker, and R. Bidarra. Generating consistent buildings: A semantic approach for integrating procedural techniques. *IEEE Transactions on Computational Intelligence and AI in Games*, 3(3):274–288, 2011. doi: 10.1109/TCIAIG.2011.2162842.

[38] A. Vaswani, N. Shazeer, N. Parmar, J. Uszkoreit, L. Jones, A. Gomez, L. Kaiser, and I. Polosukhin. Attention is all you need. *CoRR*, abs/1706.03762, 06 2017. URL `http://arxiv.org/abs/1706.03762`.

[39] C.-Y. Wang, I.-H. Yeh, and H.-y. Liao. You only learn one representation: Unified network for multiple tasks. *CoRR*, abs/2105.04206, 05 2021. URL `https://arxiv.org/abs/2105.04206`.

[40] X. Wang, J. Yi, J. Guo, Y. Song, J. Lyu, J. Xu, W. Yan, J. Zhao, Q. Cai, and H. Min. A review of image super-resolution approaches based on deep learning and applications in remote sensing. *Remote Sensing*, 14(21), 2022. ISSN 2072-4292. doi: 10.3390/rs14215423. URL `https://www.mdpi.com/2072-4292/14/21/5423`.

[41] L. Wilschut, A. Laudisoit, N. Hughes, E. Addink, S. De Jong, H. Heesterbeek, J. Reijniers, S. Eagle, V. Dubyanskiy, and M. Begon. Spatial distribution patterns of plague hosts: Point pattern analysis of the burrows of great gerbils in kazakhstan. *Journal of Biogeography*, 42, 05 2015. doi: 10.1111/jbi.12534.

[42] L. Yang, Z. Zhang, Y. Song, S. Hong, R. Xu, Y. Zhao, W. Zhang, B. Cui, and M.-H. Yang. Diffusion models: A comprehensive survey of methods and applications. 09 2022. doi: 10.48550/arXiv.2209.00796.

[43] A. Zeyer, P. Bahar, K. Irie, R. Schluter, and H. Ney. A comparison of transformer and lstm encoder decoder models for asr. *IEEE Automatic Speech Recognition and Understanding*, pages 8–15, 12 2019. doi: 10.1109/ASRU46091.2019.9004025.

[44] J.-Y. Zhu, T. Park, P. Isola, and A. A. Efros. Unpaired image-to-image translation using cycle-consistent adversarial networks. pages 2242–2251, 2017. doi: 10.1109/ICCV.2017.244.

A | Appendix A

Ripley K Histograms
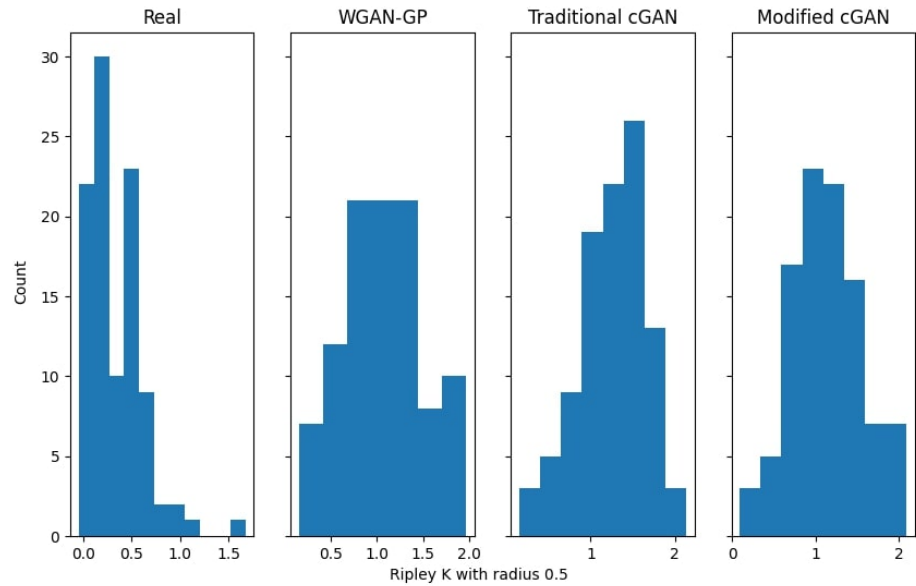
Figure A.1: Ripley K histogram with radius 0.5
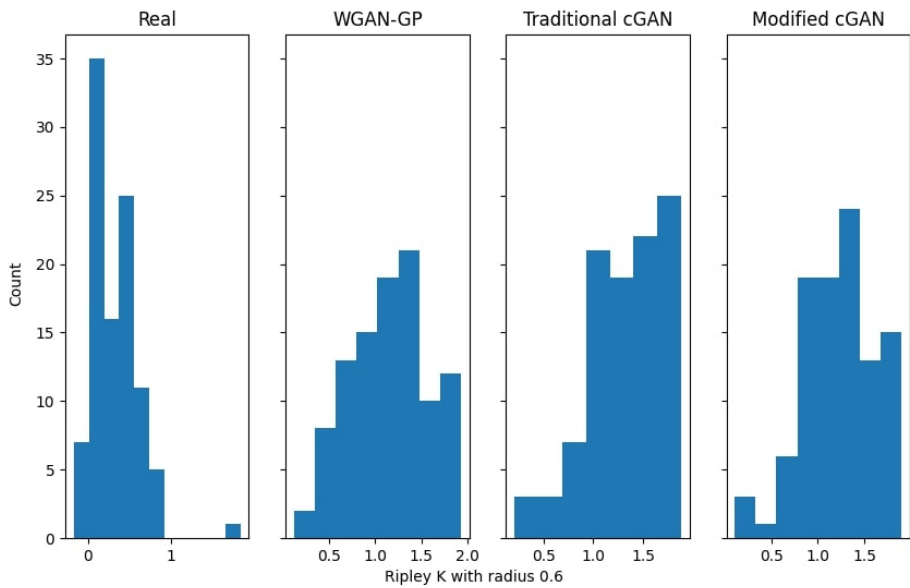
Figure A.2: Ripley K histogram with radius 0.6
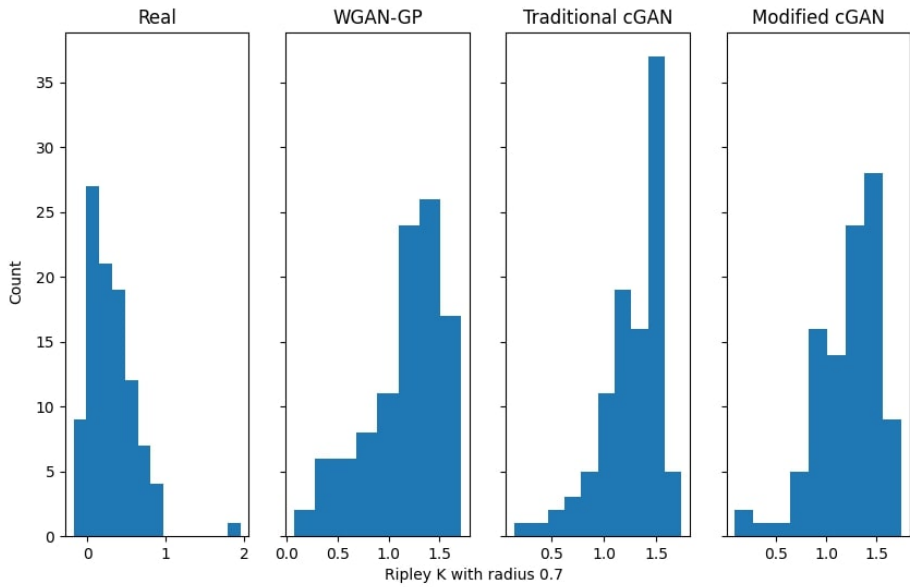
Figure A.3: Ripley K histogram with radius 0.7
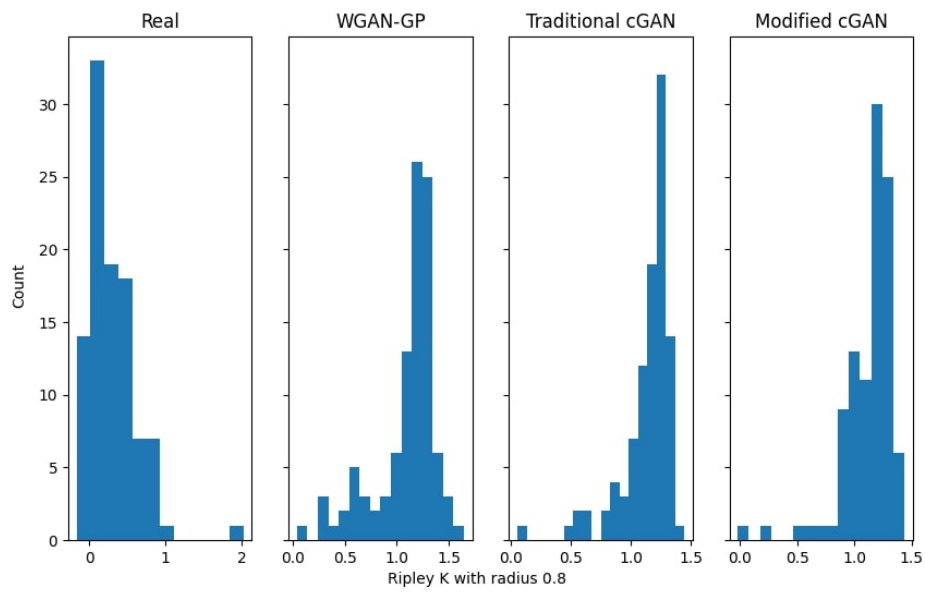
Figure A.4: Ripley K histogram with radius 0.8
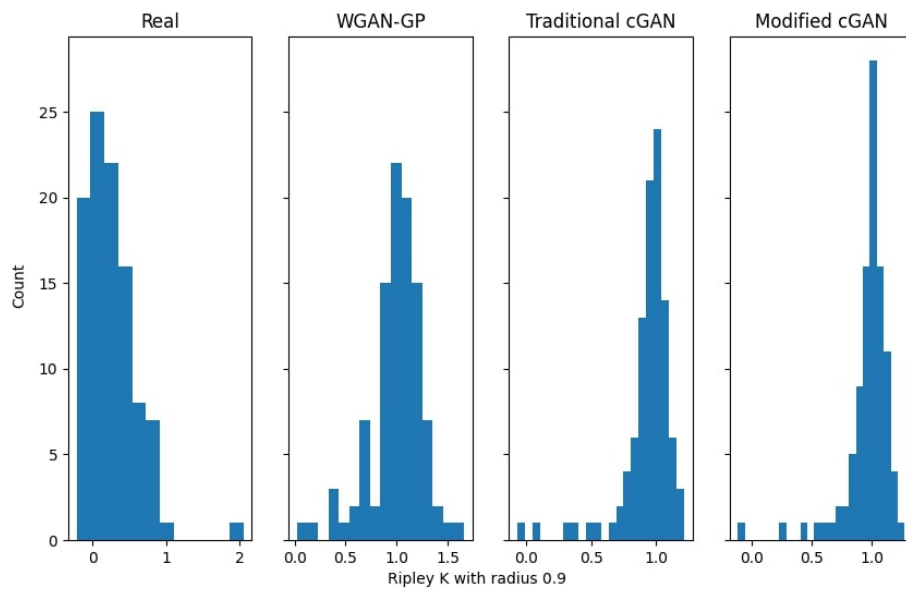
Figure A.5: Ripley K histogram with radius 0.9
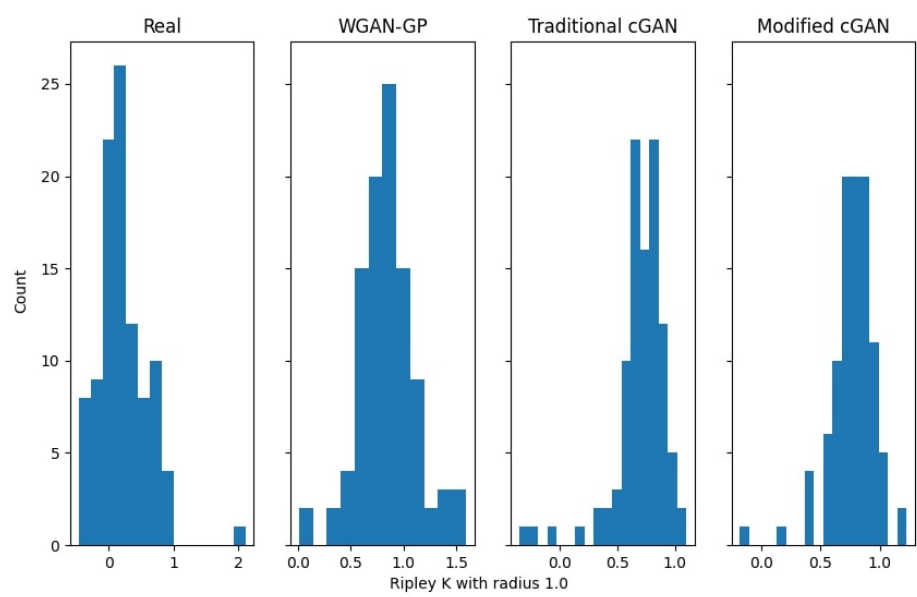
Figure A.6: Ripley K histogram with radius 1.0

B | Appendix B

Game Objects Count by Type
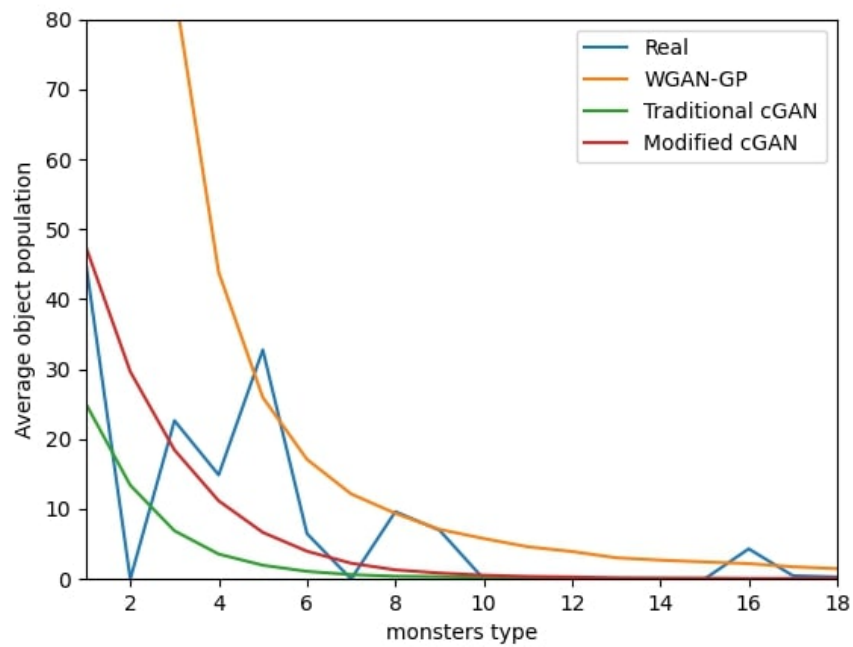
Figure B.1: Average monsters count by type in a level
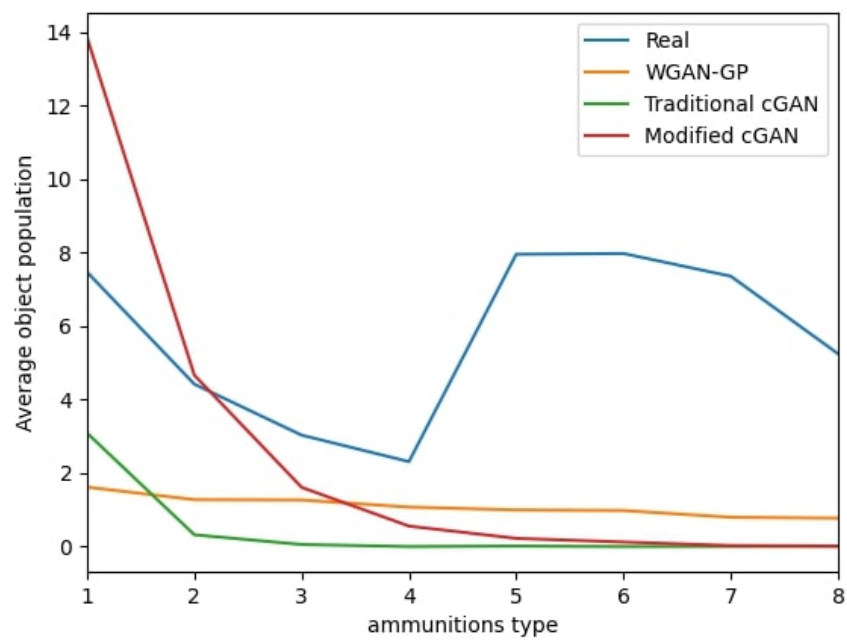
Figure B.2: Average ammunitions count by type in a level
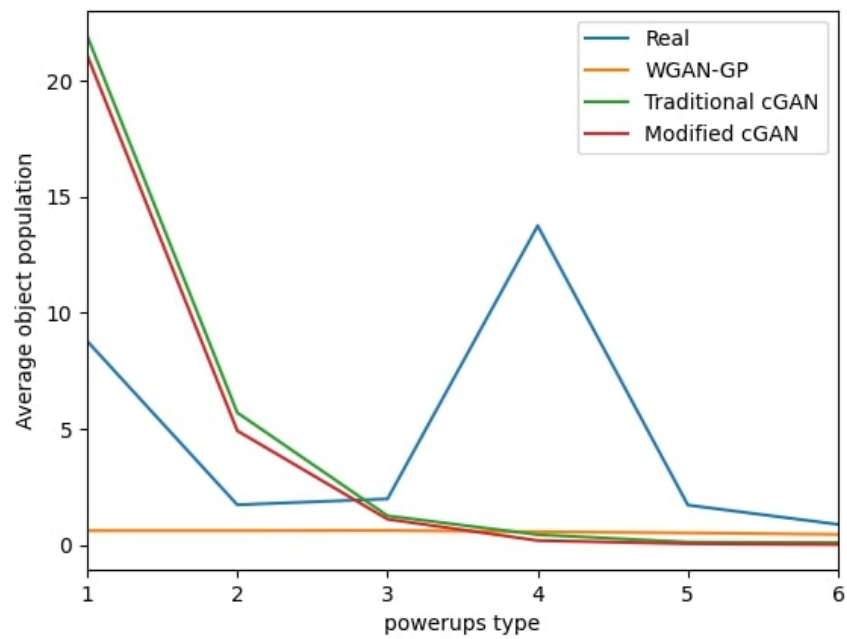
Figure B.3: Average powerups count by type in a level
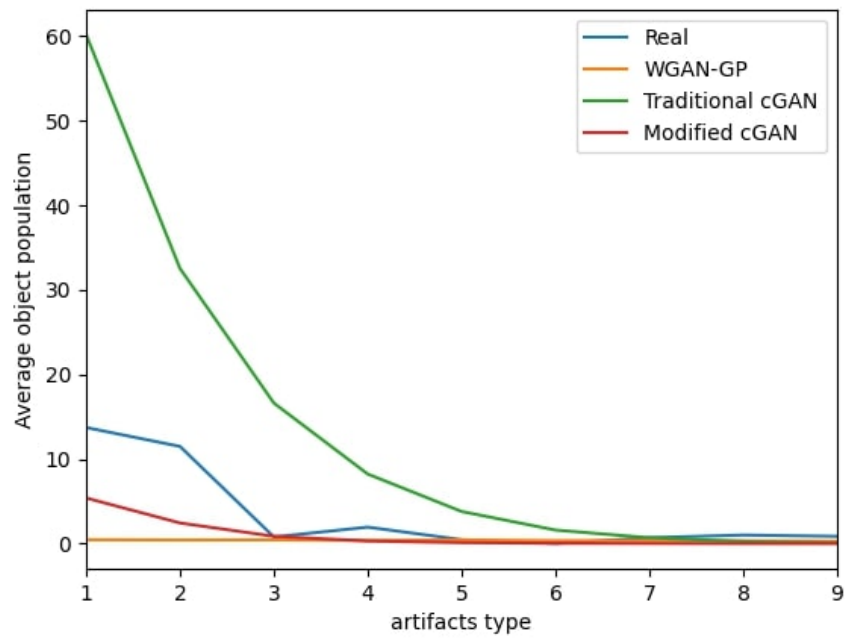
Figure B.4: Average artifacts count by type in a level
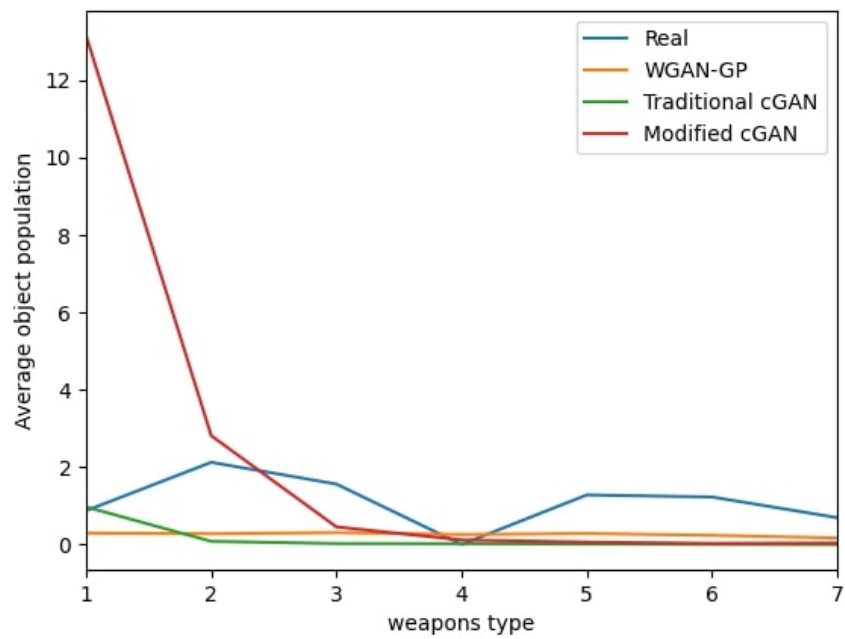
Figure B.5: Average weapons count by type in a level

List of Figures

List of Tables

Acknowledgements

I would like to thank my supervisor, Danielé Loiacono for the instructions he provided me that allowed me to write this thesis. I thank my family and friends, especially my parents who supported me both financially and emotionally through this prolonged endeavor as well as provided me with their consistent encouragement, keeping me motivated and constant reminders that helped me stay on track towards completing this thesis. I express my gratitude towards Ali Emre Soleleyuck that sat through my venting during the arising complications which let me have my breakthroughs in the most random of circumstances and Amrit A. with whom I was able to relax and redirect my focus towards actions that have been more productive.